NASA TT F-9523

HYPERLIFT AND BALANCING OF SLENDER WINGS

Ph.Poisson-Quinton and E.Erlich

Translation of "Hypersustentation et équilibrage des ailes élancées". Paper presented at the ONERA Colloquium of Applied Aerodynamics, Organized by the French Association of Aeronautics and Space Engineers and Technicians, Paris, November 12-13, 1964.

NATIONAL AERONAUTICS AND SPACE ADMINISTRATION
WASHINGTON AUGUST 1965

NATIONAL AEROSPACE RESEARCH AND DEVELOPMENT ADMINISTRATION (ONERA)

29 Avenue de la Division Leclerc Chatillon-sous-Bagneux (Seine)

HYPERLIFT AND BALANCING OF SLENDER WINGS

Philippe Poisson-Quinton and Emile Erlich

Paper read at the Colloquium of Applied Aerodynamics,

organized by the French Association of Aeronautics and

Space Engineers and Technicians (A.F.I.T.A.E.)

Paris (ENSA) 12 - 13 November 1964

HYPERLIFT AND BALANCING OF SLENDER WINGS

*/1

Ph. Poisson-Quinton and E.Erlich

14634

The problems encountered in the design and subsonic flight of supersonic transports (SST) are reviewed and calculated for slender wings, canard-type aircraft, and delta wings with and without fuselage, with and without front and aft empennage. The use of pressure-side flaps, positioned so as to avoid nose heaviness, is critically evaluated. The hyperlift created by vortex trails shed from the wing tips is used for modifying the design so as to improve the take-off and landing characteristics. Variable sweepback by use of retractable tail units permits lift increment at low speeds and better performance at Mach 2 and 3. Performance graphs for all possible designs are given.

Author

RESUMÉ

During preliminary studies for the project of the supersonic transport (SST), the National Aerospace Research and Development Administration (ONERA) has done systematic research on the lift of slender wings; the expression "slender wing" is to mean sweptback wings of the delta family, highly adaptable to supersonic flights, although their low aspect ratio gives only poor performance at low speeds.

However, the sharp sweepback of the leading edge permits an increase in

---

* Numbers in the margin indicate pagination in the original foreign text.

lift because of the development of funnel-shaped vortex streets shed from the suction side of the wing; the gain in lift will be defined as a function of the aspect ratio and of the shape of the leading edge.

The hyperlift obtainable with a slender wing is directly correlated with the possibility of stabilizing the aircraft longitudinally; several methods of balancing have been tested in the incompressible-flow wind tunnel, using "canard" type planforms or tail-controlled types, of which the advantages (magnitude of balanced lift) and the drawbacks (difficulty in longitudinal and transverse stability) as well as the computational methods will be given here; finally, we will demonstrate that it is possible to obtain a moderate hyperlift with a tailless aircraft, by using pressure-side flaps whose position is selected so as to prevent any nose-heaviness moments.

The variable-sweep wing, in principle, is truly "slender" only when flying at high speeds, while the deployment of moderate-sweepback surfaces at low speeds permits a relatively high hyperlift. However, the existence of a strongly sweptback apex produces stability problems similar to those encountered in slender wings.

1. Introduction

The increasing elongation or tapering of wings is directly connected with the development of transonic aircraft and, later, of supersonic aircraft. The attempt to reach good performance at high speeds has led to an increase in sweepback at the leading edge and to a reduction in wing thickness. Structural requirements then called for compact planforms, usually close to the delta configuration, which are familiar from the Mirages III and IV series.

More recently, ambitious civil and military programs, initiated in various

countries, have induced detailed aerodynamic research and development, resulting in projects which all have slender planforms in common (Fig.1) and where the /2 particular design was the upshoot of a difficult compromise between the contradictory requirements at low and high speeds. A brief listing of these projects is a necessary introduction to the understanding of problems raised in takeoff and landing:

a) Supersonic transport (SST), which must combine optimum aerodynamic performance at high speeds and performances at low speed at least equal to those of present-day civil aircraft. For this, two formulas have been proposed:

Tailless aircraft without hyperlift but with moderate wing loading (the Franco-Britannic projects Sud/B.A.C. "Concord" and the American Lockheed "Mach 3").

Variable-sweep aircraft with hyperlift in the configuration of "deployed wings" and tail-stabilized (American Boeing project "Mach 2.5").

b) Multimission aircraft, which meets a certain need of military authorities who are interested in avoiding multiplication of highly specialized costly types, and which is to conciliate even more contradictory performance requirements: supersonic interception mission at high altitudes, transonic attack at sea level, subsonic convoy with large radius of action, short takeoff and landing runs. This difficult aerodynamic compromise has now been realized by two prototypes:

Variable-sweep aircraft F. 111, corresponding to the T.F.X. American project.

Delta aircraft with Fowler or zap flaps and tail unit T.S.R.2, developed in Great Britain.

c) Military "Mach 3" aircraft, which have been flying for some time in the

USA; these include the experimental bomber XB 70 which is a delta-canard aircraft and the reconnaissance-interceptor YF-12A, of the tailless type.

d) Supersonic aircraft projects (long-range aircraft or first stage of a satellite booster), whose configuration cannot be accurately defined as yet; however, it is highly probable that they will be designed in the form of slender deltas.

e) Supersonic re-entry gliders, which are projects characterized by a strong sweepback at the leading edge so as to minimize the considerable heat fluxes encountered on re-entry from space. For the same reason, very blunt leading edges are desirable but these are rather unfavorable for supplementary vortical lift at high landing angles.

In our report, we will concentrate mainly on problems encountered in such slender-wing aircraft at low speeds, illustrated by several examples taken from the research done at the ONERA: We will speak of "hyperlift" with considerable reservation since it will be demonstrated that slender forms of low aspect ratio are little suitable for high lifts and even less for longitudinal balancing. Consequently, the term "hyperlift" will be used here to designate any lift increment over the value predicted by the linear theory, obtained either by the creation of a vortical flow on the suction side of the wing or by the use of flaps.

Finally, longitudinal balancing will refer here to negative lock-in of /3 ailerons, to a canard planform, or to the use of tail units. In each of these cases, we will list the stability difficulties that these devices may produce at high angles of attack.

2. Aerodynamics of the Slender Wing

Let us first assign "geometric" limits to the term "slender wing" by using

an arbitrary criterion, based on the existence of turbulence on the upper wing side. These funnel-shaped vortex trails, forming mostly near the leading edge, induce local supervelocities (Fig.2) that give rise to an additional lift which should be substantial with respect to that predicted by the linear theory. It will be demonstrated that wings of the "delta" family, with an aspect ratio below or equal to about 2.2 and having a sharp leading edge, meet this criterion.

2.1 - Figure 3 illustrates the extreme limits of the region studied here, for wings of aspect ratios of 2.2 and 0.8, respectively. It is obvious that the wing with the largest aspect ratio has a higher gradient at the origin, as predicted by the calculation, but - conversely - has a less rapid increase in the coefficient of lift C_L at high angles of attack. In fact, the two wings have almost the same C_L above 20°, because of the degradation of lift of the wing with the highest aspect ratio, produced by wing-tip stall.

An analysis of the local lift gradient (dC_L/d_i), proposed by L.Cabot to the O.N.E.R.A., is particularly useful for evaluating the extent of the "hyper-lift" vortex zone of a family of wings or, conversely, for defining the appearance of trouble connected with wing-tip stall or with an "explosion" of the vortex sheet.

The effective lift can thus be considered as being the sum of two terms: one a linear term which is readily calculated and the other a term of vortical origin, for which we will attempt to define the limits.

2.2 - The linear lift of a family of slender wings has been calculated by the method of the "lifting surface" in the three-dimensional trough of the laboratory for electric analogy (Bibl.1). Figure 4 shows the evolution of the lift gradient as a function of the aspect ratio of tapered delta wings and truncated wings of "delta" form or of "gothic" form (leading edge in the shape

of a parabolic arc). These two curves tend toward the Jones value of $C_{l_i} = \frac{\pi\lambda}{2}$ as soon as the aspect ratio tends toward zero.

2.3 - Vortical lift is correlated with the presence of a funnel-shaped vortex sheet which develops downstream of a separation point at the sweptback leading edge. This lift will appear at the inception of an incidence for a sharp leading edge, but only at a rather high angle of attack for a rounded leading edge or a leading edge cambered downward.

In the case of a thin wing with sharp leading edge, various authors (Bibl.2) have proposed formulas for deriving the vortical lift development with the angle of attack. We have used here the equation $\Delta C_{l_t} = f(\lambda^{1/3} \cdot i^{5/3})$, which is valid near a speed of Mach 1 (Bibl.19). The introduction of the ratio of the linear lift gradients in the incompressible range (electric trough) and at /4 Mach 1 (Jones), namely, $R = 4.9/(4.9 + \lambda)$, will then permit to express the total lift of delta wings at low speeds in the form of

$$C_l = k \cdot R \left(\frac{\pi\lambda}{2} \, i_{rd} + \pi\lambda^{1/3} \cdot i_{rd}^{5/3} \right)$$

where k is an empirical adaptation coefficient.

Figure 5 shows the excellent agreement of this calculation with experiments (Bibl.3), for a value of $k = 0.915$. This factor depends specifically on the thickness and type of the wing profile. The diagram also shows the importance of the vortical lift increment which here is 65% of the linear lift at an angle of approach of about 12°.

Practical experience has shown that the increase in this vortical lift is limited to angles of attack which are lower the larger the aspect ratio. This limitation becomes quite obvious when analyzing the evolution of the local lift gradient as a function of the angle of attack. Figure 6 demonstrates a common

critical value, obtained experimentally for a large number of slender planforms with sharp leading edge: $(C_{L_i o})_{loc\ max} = 0.05$. The local gradient then diminishes, at a rate which increases at decreasing slenderness of the wing (wing-tip stall or breakup of the vorticity).

Using this empirical value of 0.05 as ceiling for the local lift gradient, we calculated (Fig.7) a family of curves for the effective lift (C_L, i) for a family of delta wings with aspect ratios ranging between 0.6 and 2.9 (critical value for which no more vortex effect exists). The experimental points referring to isolated wings or to wings combined with fuselage agree well with the calculated evolution, but the "effective" aspect ratio generally is slightly lower than the geometric aspect ratio (coefficient $k > 1$).

It is of interest, based on this family of curves and the graph constructed for a family of gothic wings, to calculate the effective lift ($C_L = C_{L_\ell} + \Delta C_{L_t}$) obtainable at a reasonable angle of approach ($i = 12^\circ$) for various aspect ratios. Figure 8 shows that this calculation furnishes an evolution which is fully confirmed by numerous wind-tunnel tests with mockups. It will be noted that the presence of a fuselage on a slender wing of this type does not greatly influence the lift.

This plotting also shows that the relative gain in vortical lift is specifically interesting at low aspect ratios:

$$\lambda = 2\Delta C_{L_t}/C_{L_\ell} = 26\%$$

$$\lambda = 1\Delta C_{L_t}/C_{L_\ell} = 72\%$$

which is the basic principle that makes the projects of needle-nose flying wings such as the "Concord" useful also at low speed.

Above, we have assumed that the wing was very thin with a sharp leading edge and a symmetric profile; as soon as this is no longer the case, the genera-

tion of the vortical regime, connected with the separation of the boundary layer at the suction side, may be greatly retarded if the leading edge is rounded or cambered toward the bottom. Conversely, it is possible to increase the vortical regime at a given angle of attack. Figure 9 gives a schematic view of the configurations corresponding to one or the other case:

a) A thick slender wing with a blunt leading edge (case of the supersonic /5 glider) retains a purely linear lift up to an elevated angle of attack, which results in a considerable lift decrement with respect to the same wing of sharp leading edge. This difference is clearly shown in Fig.10, which compares the lifts of 75° gothic wings having, respectively, thick and thin profiles. It will be noted that the influence of the Reynolds number, which is negligible in the case of a sharp leading edge, becomes quite considerable in the case of a rounded leading edge since it governs the appearance of flow separation which, in turn, leads to the generation of a lift vortex. This Reynolds effect is specifically important in studies of the landing of lifting bodies on re-entry from space.

b) An "adaptation" by cambering a sharp leading edge will result in a displacement of the overall curve of the local lift gradient toward positive incidences, i.e., a lift decrement which, compared to a given approach angle, is no longer negligible. This is the price to be paid for an adaptation having the purpose of increasing the maximum fineness ratio of the aircraft within a large Mach region (gain by the "suction" effect at the leading edge near the adaptation C_L, which is considerable if the leading edge is distinctly subsonic).

c) An attractive aerodynamic solution which, however, is technically difficult, consists in making the entire leading-edge unit swivelable (Bibl.2):

either toward the bottom so as to increase the fineness ratio at coeffi-

cients of lift above the adaptation C_L;

or toward the top so as to increase the turbulent lift at a given angle of attack.

These deflections result in a displacement of the overall curve of the local lift gradient toward angles of attack that are either positive or negative. Figure 11 gives a balance of these gains, with respect to maximum fineness ratio and lift at approach, obtained on two tailless aircraft mockups balanced longitudinally. The gain in fineness ratio obtained by deflection is less than that obtained by a cambered leading edge, properly calculated for a certain coefficient of lift; a deflection toward the top of such a leading edge would also restore the vortical lift at higher angles of attack.

d) Finally, it is possible to increase the vortical regime by ejection of air over the entire span of the leading edge in the wing plane (Fig.9). Research done in the wind tunnel at Cannes has indicated that this method is specifically interesting for rounded or adapted leading edges of delta wings with strong sweepback, which become vortical already at low angles of attack. The efficiency of the system (ratio of gain in lift to thrust in the countercurrent airstream) passes through a maximum for relative-wind coefficients of the order necessary for the classical boundary-layer control on hyperlift flaps ($\Delta C_L / C_\mu \sim$ ~ 3, for $C_\mu = T_s q_0 s \simeq 0.03$).

2.4 - It is impossible to speak of slender wings without mentioning the problems of reduction in stability, frequently encountered at high angles of attack and high sideslip. With respect to longitudinal stability, there fre- /6 quently is a tendency to nose-up ("self-stall" or "pitch-up") at high angles of attack, rendering the aircraft unstable. This well-known phenomenon of swept-back wings also occurs in tapered delta wings with insufficient sweepback of the

leading edge. In this case, the vortex sheet which, at increasing angle of attack, progressively approaches the plane of symmetry (Fig.2), no longer is located at the wing tip. The resultant decrease in negative pressure then leads to a tail-heaviness moment. This is clearly indicated by a comparison of the slope of the stability curves for delta aircraft having decreasing sweepback: 70°, 60°, and 50°, which are plotted here with the same static stability margin at low angles of attack (Fig.12a). For a delta of 50°, which incidentally no longer is of the "slender wing" type, the violent pitch-up is due to wing-tip stall. For a delta of 60°, the stability loss is more progressive and becomes negligible for a delta of 70°.

A wing-tip cut-off or, preferably, an outline of the leading edge as a parabolic arc (gothic wings shown in Fig.12b) will yield perfectly linear stability curves since the vortex sheet then remains close to the wing tip at high angles of attack.

Pitch-up may also result from an exaggerated extension of an apex with strong sweepback (Fig.12c) whose vortex prematurely moves away from the wing tips. As above, the tendency to nose-up increases progressively with the angle of attack. In the present example, the "gothic" wing with a parabolic planform which has the same form in the rear plan, exhibits a slight tendency to nose-down. Therefore, it can be stated that it is possible to design an intermediary apex form, which would result in a perfectly linear stability curve.

Another method of reducing the pitch-up consists in generating a compensating pitch-down moment, by placing, below the vortex sheet, a control surface attached to the trailing edge (Fig.12d) which will be actuated by the negative pressures induced at angles of attack at which the vortex approaches the wing root. A counter sweepback, at the trailing edge, which also might reduce the

pitch-up, acts in accordance with the same principle.

Double-delta wings, with the sweepback accentuated at the apex, have been selected for certain projects so as to facilitate aircraft balancing at supersonic cruising. The load at the apex will become important at high Mach numbers, and the resultant decrease in stability will compensate the transonic rearward shift of the aerodynamic center of the simple wing. As mentioned above, these configurations are subject to pitch-up, whose intensity increases here with the size of the surface added to the nose. Figure 13 gives a typical example of the progressive tendency to nose-up, produced by a fillet of 80° sweepback, added to a delta wing of 60°. The increase in lift, resulting from this, is very slight at low angles of attack but the vortical lift becomes considerable at high angles of attack.

The same diagram shows that the basic wing (D) has a perfectly rectilinear stability curve, because of a cut-off of 20% at the wing tip. Conversely, a 10% cut-off (B) is insufficient to prevent the pitch-up connected with the decrease in wing-tip loading at high angles of attack.

Lateral flanks, extending the wing toward the upstream side along the fuselage ("planing fins", Fig.14) play the same role as nose extension, i.e., they reduce the static margin in supersonic flight. At the same time, however, they produce an increase in directional stability at high angles of attack. Here, Fig.14a shows that, in skidding flight, the vortex of the windward planing /7
fin produces intense negative pressures along the lateral flanks of the fuselage (favorable yawing moment) and on the suction side of the fin (rolling moment). This leads to a considerable increase in directional stability at high angles of attack. Unfortunately, the positive induced roll, which already is predominant in slender wing designs, is further accentuated by this device. The abrupt de-

crease in these coefficients, ΔC_n and ΔC_l, beyond 10° of sideslip (i = 18°) corresponds to a separation of the vortex sheet on the windward side of the wing, a phenomenon which will be discussed in more detail later in the text.

The lift increment and the tendency to nose-up produced by these lateral flanks (Fig.14b) will occur only at a relatively high angle of attack, despite the fact that these flanks have a sharp leading edge.

The degradation of the funnel-shaped vortex sheets, at a certain distance from their origin, is a phenomenon that is of importance only if it occurs above the suction side of the slender wing. In that case, this discontinuity in the vortical regime will result in an abrupt decrease in the negative pressures induced on the rear section and thus will lead to loss of lift and tendency to pitch-up.

For a given sweepback, this "breakaway" advances progressively from the trailing edge to the nose, with increasing angle of attack. The breakaway appears at the trailing edge at angles of incidence that are lower the more the sweepback is moderate [Figs.15a and b, according to R.A.E. tests (Bibl.4)]. If the aircraft is in a sideslip, the wing "facing the wind" which has the less effective sweepback is the first to be struck by this breakaway, resulting in an abrupt decrease in roll and in directional stability (see Fig.14a).

A typical example for this phenomenon, observed on a special wing with double sweepback (delta 60°, with an 80° sweepback nose) at the Cannes wind tunnel, is given in Fig.15c. The course of the wall flow, at two adjacent high incidences, makes it possible to localize this breakaway, which results in an abrupt drop in lift and a violent pitch-up. Let us mention that the visualization in the hydrodynamic tunnel is in complete agreement with the wind-tunnel results.

3. Hyperlift of Slender Wings

A strong hyperlift, comparable to that obtained with present-day aircraft of high aspect ratio, is out of question for slender wings, for the two following reasons:

The efficiency of a flap decreases with the aspect ratio of the wing;

The nose-heavy moment, produced by the deflection of the flap, is relatively high because of the large lever arm between the center of gravity and the center of application of the supplementary lift. In this case, compensation of a strong hyperlift is impossible with empennages located at reasonable distances forward or aft of the fuselage.

The problem of longitudinal balancing is thus more restrictive in this case than that of the intrinsic efficiency of a hyperlift device.

3.1 - A calculation of the influence of flaps on slender wings presents /8 no difficulty. The rheoelectric method is still of great value in this case, for determining not only the efficiency of a flap or of an elevator or roll stabilizer but also the location of the center of thrust of the lift variation (secondary a.c.). Figure 16 shows the excellent agreement between this calculation made on an isolated wing in the electric trough and the full-scale mockup tests in the wind tunnel.

On this example of a gothic delta wing with moderate sweepback, it was found that, for a center of gravity located, for example, at 50% of the mean chord (static margin of 3.5%), the center of application of ΔC_L is located at 80%, i.e., quite far in back of the chord. To balance the nose-heavy moment of a hyperlift flap, by using a tail unit mounted near the trailing edge or near the leading edge, one could be tempted to elongate such a slender-wing aircraft excessively, which it already had been by definition. Conversely, in the absence

of hyperlift, the balancing of a tailless aircraft requires only slight negative deflections if the static margin is low.

3.2 - The selection of the type of hyperlift flap depends on the desired ΔC_L (Fig.17).

A slotless flap, on a classical 60° delta wing (Fig.17a) has an efficiency which agrees satisfactorily with the calculation (Bibl.5) up to about 15° deflection. A slot permits extending this agreement up to 30°, with the efficiency passing through a maximum near 45° deflection. Practical experience has also shown that an increase in the span of the flap, which in principle is of interest for the increment ΔC_L, unfortunately leads to a prohibitive overload at the wing tip which stalls prematurely as soon as the low angles of attack result in a longitudinal instability (pitch-up).

A reduction in wing span (aspect ratio changing from 2.18 to 1.34 by truncating the wing tip), for a given hyperlift flap will result in a considerable loss of efficiency (Fig.17c) which could then be minimized by using wing-tip disks which increase the effective aspect ratio.

The problem of boundary-layer control by flaps is well known (Bibl.6, 7, and 8) and is used in numerous aircraft. The example shown in Fig.17b, referring to a 60° delta wing with pressure slots, tested at the R.A.E. for use in the T.S.R.2 supersonic aircraft, showed that such ejection of an air jet will restore the flow on the flap [ΔC_L equal to that calculated for a perfect fluid by a method given elsewhere (Bibl.5)] for values of the suction factor which increase with the deflection (here, $C_\mu \cong 0.01$ for $\alpha_v = 50°$). This boundary-layer control by pressure slots (compressed air tapped from the jet-engine compressor) readily permits a doubling of the lift of a "slim" aircraft at landing incidences. In fact, in the very thin wings of supersonic aircraft it is easier

to install high-pressure suction ducts ending in rotating flaps than to install the complicated kinematic system of classic slotted flaps with recoil.

More intense ejection of air (control of the circulation) can be obtained by deflecting the engine jets, as discussed below (Fig.28).

4. Longitudinal Stability of Slender Wings /9

Let us first review briefly the three principal methods of longitudinal balancing for the simple case of a schematic aircraft without hyperlift:

In Fig.18, three different aircraft configurations are given:

without tail unit (flying wing);

with rear tail unit;

with canard-type empennage.

The centers of gravity of these tail units were so arranged that the static margin was the same (aerodynamic center at 3% of the mean chord aft of the center of gravity). The balancing, at a given angle of attack, is obtained by deflecting the control surface which leads to a loss in coefficient of lift for tailless aircraft with rear tail unit but to an increase in coefficient of lift for a canard aircraft:

$$\Delta C_L = (d_f / d_{fs}) \cdot C_L \text{ (not balanced)}$$

where d_f and d_{fs}, respectively, are the distances from the center of gravity to the focus of the aircraft and to the secondary focus of the control surface. In the actual case, a tailless aircraft will suffer a lift decrement, due to the balancing, of $-\Delta C_L = 12\% C_L$, while an aircraft with a rear tail unit will have a loss in lift of only 4% and the canard-type aircraft will have a gain in lift of 3.2%.

4.1 Tailless Aircraft

4.1.1 - To reduce the lift decrement, due to the balancing of an aircraft without tail unit, one possibility is to reduce the static stability margin to a minimum. In this direction, however, a limit is produced by the necessity of maintaining stability up to the highest angles of attack useful to a given aircraft. If the stability curve is not linear but, as frequently is the case in slender wings, shows a tendency to nose-up at high lifts, the static margin will be excessive in cruising flight, resulting in an increase in balancing drag. In this respect, it should be recalled that the balancing drag can be considerably reduced because of the existence of a law of spanwise camber and twist of wing profiles (Bibl.9 and 10) in such a manner that the aircraft is self-balanced at the cruising C_L, without deflection of the control surface (for example, the "Concord" project). The weak tail-heavy moment C_{m_0}, resulting in this case, is generally insufficient for balancing the aircraft on takeoff and landing.

4.1.2 - Strongly cambered forms are desirable for blunt lifting bodies during re-entry from space so as to ensure their longitudinal self-balancing at high angles of attack. Figure 19 shows the aerodynamic characteristics of such a supersonic glider at landing speeds. On the gothic wing with rounded leading edge, the vortical lift appears only near an angle of attack of 5°. An installation of fins at the wing tip will increase the lift gradient at the origin (increase of the effective aspect ratio by a "panel" effect) but counteracts the development of vortical lift (Fig.19a). Such double fins will reduce the longitudinal stability but will make the curve (C_L, C_m) practically linear at a C_{m_0} sufficiently high to ensure a self-balancing near angles of attack of 10°. The longitudinal control, in this case, will then require only negligible deflections

of the elevons (Fig.19b). Of interest is also the relatively high value of the maximum fineness ratio for a body of such low aspect ratio, which renders it "landable".

As in all wings with strong taper, the roll induced by the sideslip is /10 quite considerable but control in roll is facilitated by differential deflection of the elevons (Fig.19c). Finally, the directional stability increases with the incidence in this particular configuration with lateral fins (Fig.19d).

4.1.3 - It is well known that the hyperlift efficiency of a pressure-side flap diminishes as soon as its hinge advances toward the leading edge (Fig.20). However, a moderate gain in lift is of great importance if the pitching moment created is either zero or a fortiori of the tail-heaviness type, when used for a tailless aircraft. Practical experience has shown that an optimum placement in depth exists, leading to a maximum lift increment without modification of the pitching moment. A gain in lift of 18% at the approach angle has been obtained for a specific configuration of a strongly deflected flap. This device would also produce a 50% increase in aircraft drag, which has a favorable influence on the reduction of the rate of entry into the range of velocity instability ("second regime" or stalled condition). This velocity instability, which is an inherent drawback of tailless aircraft with tapered wings, due to their low fineness ratio, can be kept to a tolerable value by a suitable adaptation of the jet-engine regime to the kinetic flight pressure.

4.2 Canard Aircraft

The principle of longitudinal stabilization of a hyperlift wing by a canard design is quite attractive, since a part of its inherent lift is added to that of the flaps and since its lever arm, with respect to the center of gravity,

can generally be greater than that of a rear tail group. However, this configuration has been used only in rare cases, for various reasons of which the most important are as follows:

Increase in structural weight of the fuselage nose which must be reinforced to carry the loads of a canard design.

Interactions due to the vortices shed by the canard design and reaching either the wing at a certain incidence (loss of longitudinal stability) or the fin at a certain sideslip (loss of directional stability). Below, we will list methods for minimizing these interactions.

4.2.1 - The ONERA has done extensive basic research on the calculation and testing of canard-type empennages, useful for rockets or aircraft. We will merely list some of the results of these calculations for incompressible flow:

a) Lift of a canard planform: Figure 21 gives a comparison of computational and empirical data for a combination of swivelable canard fuselage with respect to the lift gradients obtained, respectively, by effects of angle of attack and flap deflection. The lift gradient of the canard type, in the presence of a fuselage, has been calculated on the basis of the lift of an isolated canard and of the coefficients of reciprocal interaction, based on the theory of slender bodies (Bibl.11, 12). This calculation is in satisfactory agreement with the experimental results obtained by difference measurements of (fuselage + + canard) and (fuselage alone) configurations.

b) The calculation of the pitching moment, applied to the canard planform, is obtained on the basis of the theory for slender bodies. To avoid long calculations, it is assumed that the negative lift induced by the canard planform on the wing (Bibl.13) is applied at the center of gravity of the evolutional part of the wing section exposed to the vortex sheet shed from the canard /11

(Bibl.14). Figure 22 gives a comparison of calculation and experiments for two configurations of a delta-canard aircraft with 60° sweepback, on which either the lever arm or the surface of the canard planform were varied. This calculation, performed on the basis of experimental data obtained on the (wing + fuselage) configuration agrees satisfactorily with the tests.

c) Proceeding from the above computational methods, it is possible to obtain an approximate definition of the positioning and the size of a canard plane, capable to compensate a certain hyperlift output. Figure 23 indicates the efficiency of a pivoting or swivelable canard (rated here in degree of deflection per unit ΔC_L, furnished by the hyperlift flap) as a function of the lever arm and of the dimensions of the canard. It will be noted particularly that an increase in span or an increase in the lever arm will no longer be profitable above certain, relatively moderate, values. In subsequent tests, we adopted a canard span equal to three times the diameter of the fuselage and used a distance between trailing edges about 1.7 times that of the mean chord of the wing.

4.2.2 - A systematic experimental study of the balancing of classic slotted flaps was conducted on an aircraft mockup with a 60° delta-gothic wing, with conical camber in the median position along the fuselage. Successive experiments were made with swivelable, floating, and fixed canard planforms with suction flaps. The comparative results are presented in Fig.24 in the form of balanced lifts obtained for one and the same static margin (4.3% of the mean chord). In each case, the canard remained at a locked-in deflection at variable incidence, and the balancing was obtained by varying the deflection of a flap acting as "elevon".

a) The swivelable canard was of the type analyzed previously (Fig.23). Its

balancing power was limited by its possible stall at combinations of angles of attack and deflection that approach the maximum coefficient of lift for a 60° delta plane. This drawback is clearly indicated in Fig.25a, where the lift of the swivelable canard is plotted as a function of the angle of attack for two extreme deflections of 0° and 15°. At a relatively high angle of attack of i = = 15°, it is obvious that the increment ΔC_L, useful for the balancing, is limited by its maximum lift (i + β = about 30°).

b) The principle, if not its actual construction, of a "floating" canard is quite attractive. This type is free to pivot about a hinge and its setting is controlled by a small flap (trailing-edge "tab"). Consequently, for a given position of this flap, the lift obtained on the right of the swivel axis is almost independent of the incidence, so that the prime advantage of a floating canard is that of being "transparent", i.e., its presence produces practically no changes in the static margin of the (wing + fuselage) configuration, which permits a more rearward shift of the center of gravity than in the case of the preceding design. This will lead to a larger lever arm for the canard type aircraft and a smaller lever arm for the hyperlift flap.

Its second advantage lies in the fact that the useful lift for balancing is much greater than that of the swivelable canard whose angle of deflection is limited by the breakaway (function of i + β) since here the entire lift at /12 high incidences can be utilized. Figure 25b shows that, under these conditions, one is no longer limited by the $C_{L\ max}$ of the delta type at high angles of attack. This double advantage, in the presented example, leads to a considerable increase of the available tail-heavy moment, of the order of 2.2 times that possible with a swivel canard.

The "floating" canard, fixed at the instant of piercing the sonic barrier,

permits a reduction in the excess static margin of the aircraft in the supersonic range, which constitutes still another advantage.

However, it is obvious that such a device will require considerable supplementary research, specifically as to its dynamic behavior and to the possible transonic difficulties expected from such a "floating" configuration.

c) The canard with pressure slots, tested here and having a lozenge planform, is mounted to the upper portion of the wing with a positive dihedral of 15° so as to remove the resultant vortices as far away from the plane of the median wing as possible. Only the control surface is movable, producing a tangential ejection of air, which permits restoration of smooth flow at high deflections. The lift efficiency of this canard with pressure slots, namely, the ratio of lift increment ΔC_{L_c} to available thrust (coefficient C_μ of air ejection) is of the order of 6 in the example given in Fig.24. The curve of the lift, balanced by pressure slots on the control surface deflected by 60°, corresponds to a constant thrust of the air compressor such that $C_\mu / C_L = T_s / P = 0.015$. There is a lack of linearity of the curves for the lift and for control at low angles of attack, which is a phenomenon due to a vortical interaction which will be discussed later in the text.

The comparison sheet of the balanced hyperlift of the three above solutions, at an approach incidence of 12°, with the value obtained for a tailless aircraft at the same static margin, indicates increasing gains, as follows:

	$C_{L_c}(i = 12^{\circ})$
Tailless aircraft	0.39
Aircraft with swivel canard	0.63
Aircraft with floating canard	0.73
Aircraft with pressure-slot canard	1

These impressing lift increments over tailless aircraft obviously are accompanied by an increase in the maximum fineness lift, resulting in a notable reduction of the velocity of entry into the second regime during the approach flight.

4.2.3 - The regime of intense vorticity in the downwash from the deflected canard unfortunately interferes with both longitudinal and transverse stability, which may have serious results in cases of poorly investigated configurations.

a) Typical perturbations, observed with respect to the longitudinal stability of two configurations of canard aircraft with pressure-slot control are shown in Fig.26.

In the case (a) of a median wing with positive setting and a low position of the canard control surface, the sharply deflected vortex sheet shed by the /13 canard approaches the underside of the wing only near an angle of attack of 7°. At this instant, the local supervelocities induced by the vortex at the pressure side of the wing will result in a loss of lift and a violent tail-heavy moment, which makes this configuration useless at angles of attack between 7° and 12°.

The configuration (b), conversely, uses a canard with pressure slots, placed high on the fuselage at a positive dihedral. In this case, the vortex sheet strikes the pressure side of the wing at the median position, starting from very low angles of attack; these perturbations disappear again at an angle of 5° at a time at which the vortex sheet has passed to the suction side of the wing (at this instant, the induced supervelocities result in a supplementary lift and in a nose-heavy moment).

A more detailed investigation showed that these perturbations can be neglected at still lower angles of attack (i.e., outside of the domain of approach flight) for a wing of low position.

b) The perturbations observed with respect to transverse stability also originate in the vortex sheet which, this time, forms at the fins. Figure 27 illustrates this phenomenon for the case of an aircraft with swivelable canard (deflected at 15°) in sideslip: At an angle of attack of 15°, the vortex sheets form at the suction side of the wing and thus strike the fin (or fins).

In the case of a single-fin aircraft, the vortex system induces supervelocities which produce an unstable moment which lasts until the angle of sideslip becomes sufficiently large to have the two vortices be located on the same side of the fin. The moment, due to the induced negative pressures, will then become favorable.

In the case of a two-fin aircraft where the fins have a spacing equal to the span of the canard control surface, the phenomenon is exactly opposite since, at zero sideslip, the two vortices are located between the fins. Thus, the directional stability is excellent until the two vortices pass along the outside of one of the fins toward $j = 8^{\circ}$, which again will lead to directional instability. Let us recall that these upper-side fins may cause a violent pitch-up if they are installed in the path of the vortex sheet shed by the wing, i.e., too close to the wing tips.

Finally, this same Fig.27 shows that the presence of a canard control surface, in the absence of fins, is of benefit for the directional stability at low angles of attack because of the supervelocities induced by the vortices along the flanks of the fuselage. This phenomenon is similar to that mentioned above for the lateral flanks of the fuselage (Fig.14).

4.2.4 Balancing by Jet at the Fuselage Nose

The present development of very light-weight lift jets for certain V.T.O.L.

aircraft promises their later use for the longitudinal balancing of hyperlift devices in aircraft with slender wings. The lift efficiency is quite inferior to that of a canard with pressure slots but such a simple jet will produce no /14 perturbation of the aircraft stability (Bibl.15).

As a typical example, we are giving here an evaluation of the thrust required at the front of the fuselage for compensating a strong hyperlift.

Figure 28 presents results of the lift and moments obtained in the Cannes wind tunnel with a 60° delta aircraft mockup, equipped with a central pressure flap. To minimize the nose-heavy moment and to increase the efficiency of the flap, the latter was placed in front of the trailing edge between fins, forming panels. The pressure coefficients used here are quite superior to those required for re-attachment of the boundary layer and correspond to an extensive control of circulation (Bibl.2). Deflections of the flap up to 90° will become possible and the coefficients of lift obtained are very high for a wing of such low aspect ratio: $C_{L_W} = 3.2$ for $C_{\mu_W} = 1.7$ at $i = 0^{\circ}$. Calculation shows that the thrust produced by the vertical jet at the fuselage nose, for compensating the nose-heavy moment, corresponds to $C_{\mu_N} = 0.38$ which is added to the preceding C_{L_W} to yield a total compensated lift of $C_{L_T} \cong 3.6$ at zero incidence. This total mechanical equipment represents about 58% of the aircraft weight, of which 20% are taken up by the balancing jet. These orders of magnitude are not prohibitive for an S.T.O.L. aircraft designed for supersonic flight.

Less extensive hyperlifts, corresponding to a positive deflection of the order of 5° of a classic elevon, can be compensated by thrusts (assumed as being applied at a distance equal to one mean chord, forward of the center of gravity) constituting less than 7% of the aircraft weight. The resultant lift increment at approach, with respect to the tailless aircraft, is of the order of 40%.

The thrust of the nose jet obviously must be kept under control at the approach incidence so as to avoid a reversal of the direction of the elevon control, which would result from a constant thrust of the balancing jet.

4.3 Aircraft with Rear Tail Group

The calculation of an aircraft with rear tail unit of a slender wing is difficult because of the more or less intensive interaction of the vortices shed by the wing, depending on the position in height and the rearward shift of the tail group. Therefore, systematic tests were made at the ONERA to attempt the derivation of certain general laws and to study the longitudinal perturbations that a rear tail unit might exert on the aircraft.

4.3.1 - The variation in the experimental position of the a.c. with the lever arm of a tail group, in a position slightly lower than the wing, is given as a typical example in Fig.29a, for an aircraft with 60° delta-gothic wings. The experimental values are in satisfactory agreement with a calculation made on the basis of test data obtained for the (wing + fuselage) configuration, making use of experimental laws of deflection and lift of the isolated tail unit.

4.3.2 - An increase in the lever arm permits a balancing of higher lifts for one and the same tail unit. Figure 29b shows the lift increment obtained for the same static margin with respect to a tailless aircraft compensated by negative elevons. For a tail unit, placed close to the trailing edge of the wing assembly, the increment is even greater (of the order of 40%, for this particular static margin of 5%).

4.3.3 - The influence of the position in height of the tail group is /15 illustrated, in Fig.30, by the slope of the longitudinal stability curves ob-

tained in this case:

In the low position, the presence of a tail unit results in a considerable increase in stability, because of the value of the prevailing mean deflection.

For a position of the tail unit at midheight of the fin, the stability decreases greatly at low angles of attack (becoming close to that without tail group) because of an increase in deflection; in addition, a pitch-up appears as soon as moderate angles of attack are reached.

For still higher positions of the tail group, the stability at low angles of attack increases again but the abrupt tendency to pitch-up persists, due to the influence of the vortex field of the wing assembly.

4.3.4 - In the above example, the aircraft had a slender wing of the gothic type whose stability curve is correct. It is of interest to mention here the case of a swallow-tail wing with a strong intrinsic pitch-up (Fig.31). This drawback was first encountered several years ago, in the stage of the advance project of the experimental "Deltaviex" aircraft of the ONERA. At that time, wind-tunnel experiments showed that a low position of the tail unit permits a perfect balancing of the tail-heavy moment which occurs at angles of attack above 10° (Fig.31a).

The hyperlift of this aircraft was relatively easy to achieve and produced no trouble in longitudinal stability. Figure 31b gives a typical example of the balanced lift increment, obtained with a moderately deflected flap, first without and then with tangential air-jet ejection. In the latter case, the curve for elevator control is perfectly linear.

4.3.5 - Finally, cases exist in which the pitch-up of the wing is due to deflection of the hyperlift flaps (wing-tip stall at high overloads). Figure 32

shows that a tail group in low position will lead to a reversal of this pitch-up tendency, because of the reduction in the mean deflection starting at the angle of incidence at which pitch-up occurs (the loss in efficiency of the flap, at high angles of attack, contributes to this favorable reduction in deflection).

5. Variable-Geometry Aircraft

Variable geometry is a highly acute subject, which is mentioned here because of its possible application to aircraft with slender wings for improving either the performance at high speed or the performance at subsonic and low speeds.

The rearward shift of the aerodynamic center in the transonic range leads to flights that are too stable in supersonic cruising. This can be compensated either by a suitable transfer of fuel which will shift the center of gravity rearward (case of the Concord aircraft) or by a variable geometry based on the following principles:

a) Lock-in of a canard control surface which had become "floating" /16
in the subsonic range.

b) Downward swivel of the wing tips (case of the XB-70) which, at the same time, permits a reduction in the longitudinal stability and an increase in the directional stability, which generally is critical on approaching Mach 3.

c) Retraction of a rear tail unit which, at low speeds, permits balancing of a certain hyperlift of the aircraft.

In addition, a variable-sweep wing conciliates the strong sweepback and the low aspect ratio desirable in flights at high speed with the large aspect ratio desirable for flights at low speed.

Only two cases of variable geometry will be discussed below, namely, retractable tail unit and sweptback wing.

5.1 - Experiments were conducted on a schematic retractable rear tail unit (Bibl.16) in the Cannes wind tunnel, using an aircraft configuration with slender wing (Fig.33).

The partial retraction of this tail unit (sweepback changing from 15° to 105°) shifts the aerodynamic center forward by 3.6% of the chord, i.e., by about 2/3 of the shift for compensating the transition to the transonic regime (Fig.33a). The additional advantage of such a tail unit, extended at low speeds, is its ability to compensate the nose-heavy moment of a moderate hyperlift on the wing. The balanced lift increment, with respect to a tailless aircraft of the same static margin, is of the order of 27% at an approach angle of 12° (Fig.33b). Optimum performance is obtained by replacing the slotted control surface of the tail unit by a Fowler flap which is less cumbersome and more efficient. Here again, this hyperlift permits a considerable reduction of the velocity of entry into the second regime (by 70 knots, for a wing loading of 200 kg/m^2 on landing; Fig.34c).

5.2 - The principle of a variable-sweep aircraft is well known [(Bibl.17, 18) and Fig.34].

Because of the articulation of the wing about a pivot, conveniently positioned along the span, the advantages of a wing with strong sweepback at high speeds [supersonic cruising, transonic sea-level flight less susceptible to gusts because of the low $(C_{l_1})_o$ of a very slender wing] can be conciliated with the advantages of a wing of large aspect ratio and slight sweepback (satisfactory subsonic fineness ratio, strong hyperlift at low speeds). Intermediary sweepbacks, in addition, permit an optimizing of the flight in the higher sub-

sonic range (for example, sweepback of 45° at $M \cong 0.9$).

In configurations for low-speed flights, the strong sweepback apex forward of the deployed wing raises difficult problems of longitudinal stability because of the vortical regime which usually prevails at high angles of attack. A continuous increase in local lift at this apex results in a progressive lift decrement on the deployed wing, at increasing angles of attack. This leads to a pitch-up tendency, which is greater at sharper sweepback of the fillet (Fig.34b). This drawback can be partially compensated by a reduction in sweepback of the fillet (which is unfavorable at high speeds) or by any of the above-mentioned devices for reducing the vortical lift at the apex (cambered leading edge, /17 of the swivelable or rounded type; Fig.9) combined with antistall devices at the leading edge of the deployed wing. Such leading-edge tabs are indispensable for utilizing the hyperlift of the cambered flaps up to the permissible angles of attack for approach flight (Fig.34c).

Such an adaptation of the profiles - in supersonic cruising in the retracted position and in subsonic flight in the more or less deployed position - is not necessarily incompatible since calculation in both cases results in leading edges with camber increasing toward the wing tip.

6. Conclusions

The recent development of supersonic aircraft has resulted in a novel aspect of aerodynamics, one of whose main objects is the study of slender wings in incompressible flow.

We have shown that these wings with strong sweepback and low aspect ratio, desirable for good performance in the supersonic range, have rather poor aerodynamic characteristics at low speeds.

However, sufficient lifts and good flight qualities may be obtained at takeoff and landing angles of attack if the additional vortex lift is fully utilized, permitting properly designed slender planforms.

With respect to the useful hyperlift, this problem is intimately connected with the possibility of compensating the nose-heavy moments produced by deflection of the flaps.

For a tailless aircraft, a ventral flap is proposed which is quite inefficient but does not produce nose-heavy moments that must be compensated.

The solution of using a canard empennage is attractive with respect to longitudinal balancing but results in considerable perturbations of the longitudinal and transverse stability which, however, can be avoided by careful and detailed wind-tunnel tests.

Balancing by use of a rear tail unit is less efficient but permits satisfactory flight qualities if the positioning of this empennage is carefully selected.

Variable sweepback is mentioned here only with respect to slender wing forms. As a typical example, we demonstrated the operating principle of a retractable tail unit, placed in the rear of a flying wing or of an aircraft with variable sweep. These two configurations yield interesting hyperlift solutions and also increase the performance of the aircraft at high speeds.

Experiments and tests have shown that the successful development of a supersonic aircraft will require extremely detailed experimental investigations in the domain of low subsonic velocities.

BIBLIOGRAPHY /18

1. Malavard, L., Duquenne, R., Enselme, M., and Grandjean, G.: Properties

Calculated for Delta Wings with or without Gaps; Calculation by Electric Analogs (Propriétés calculées d'ailes en delta échancrées ou non - Calcul par analogies électriques). ONERA, Note Tech. No.25, 1955.

2. Poisson-Quinton, Ph.: Some Aerodynamic Problems of the Supersonic Transport at Low Speeds (Quelques problèmes aérodynamiques posés par l'avion de transport supersonique aux basses vitesses). ONERA, Recherche Aéronautique No.82, 1961.

3. Squire, L.C. and Capps, D.S.: Experimental Investigation of the Characteristics of an Ogee Wing from M = 0.4 to M = 1.8. RAE, Tech. Note Aero No.2648, 1959.

4. Earnsshaw, P.B. and Lawford, J.A.: Low-Speed Wind Tunnel Experiments on a Series of Sharp-Edged Delta Wings. RAE, Tech. Note Aero No.2750, 1961.

5. Lawry, J.C. and Polhamus, E.C.: A Method for Predicting Lift Increments due to Flap Deflection at Low Angles of Attack in Incompressible Flow. NACA, Tech. Note No.3911, 1957.

6. Carrière, P., Eichelbrenner, E., and Poisson-Quinton, Ph.: Theoretical and Experimental Contribution to the Study of Boundary-Layer Control by Pressure Slots (Contribution théorique et expérimentale à l'étude du contrôle de la couche limite par soufflage). First International Congress of Aeronautical Sciences, Madrid 1959; Pergamon Press.

7. Lachmann, G.V.: Boundary Layer and Flow Control, its Principles and Application. Pergamon Press, 1961.

8. Williams, J. and Butler, S.: Aerodynamic Aspects of Boundary Layer Control for High Lift at Low Speed. RAE, Tech. Note No.2858, 1963.

9. Bevierre, P.: Aerodynamic Characteristics of a Wing-Fuselage Assembly in /19 the Vicinity of Sonic Velocity; Research on Optimal Configurations

(Caractéristiques aérodynamiques d'ensemble aile-fuselage au voisinage de la vitesse sonique; recherche de configurations optimales). ONERA, Recherche Aéronautique, No.84, 1961.

10. Fenain, M. and Vallée, D.: Application of the Theory of Homogeneous Flow to the Research on Adaptation of Certain Wings in the Supersonic Regime (Application de la théorie des écoulements homogènes à la recherche de l'adaptation de certaines ailes en régime supersonique). ONERA, Memo Technique No.84, 1961.

11. Spreiter, J.: The Aerodynamic Forces on Slender Plane and Cruciform Wing and Body Combinations. NACA, Report No.962, 1950.

12. Dugan, W. and Hikido, K.: Theoretical Investigation of the Effects upon Lift of a Gap between Wing and Body of a Slender Wing-Body Combination. NACA, Tech. Note No.3224, 1954.

13. von Baranoff, A.: Nonlinear Forces and Moments Induced by a Front Wing on a Rear Wing and the Fuselage, in a Slender Configuration (Forces et moments non-linéaires induits par une aile avant sur l'aile arrière et la fuselage, dans une configuration élancée). ONERA, Note Tech. No.58, 1960.

14. Erlich, E.: Experimental Contribution to the Calculation of Configurations of the Canard Type (Contribution expérimentale au calcul de configurations du type canard). ONERA, Recherche Aéronautique, No.75, 1960.

15. Poisson-Quinton, Ph. and Bevert, A.: On the Use of Propulsive Jets at Hyperlift of an Aircraft (Sur l'utilisation des jets propulsifs à l'hypersustentation d'un avion). Technique et Science Aéronautiques, No.5, 1959.

16. Poisson-Quinton, Ph. and Erlich, E.: Variable Geometry Applied to a Tail Unit (Géométrie variable appliquée à un empennage). ONERA, Recherche Aéronautique, No.94, 1963.

17. Baals, D. and Polhamus, E.: Variable Sweep Aircraft. Astron. and Aerosp. Eng., June 1963.

18. Alford, W. and Driver, C.: Recent Supersonic Transport Research. Astron. and Aeronautics, Sept. 1964.

19. Legendre, R.: ONERA, Recherche Aéronautique, Nos.30-31, 1953.

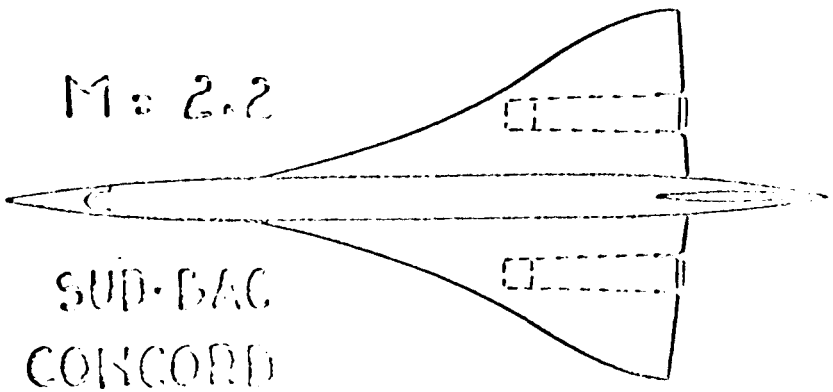

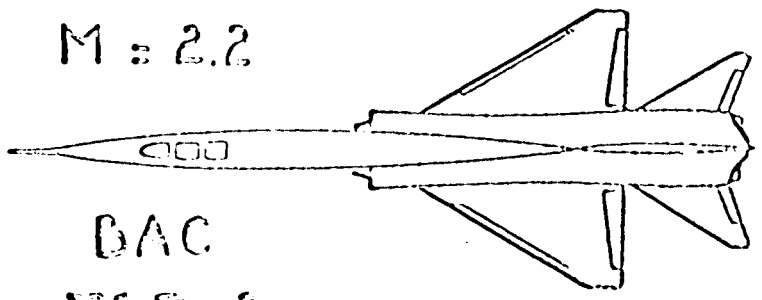

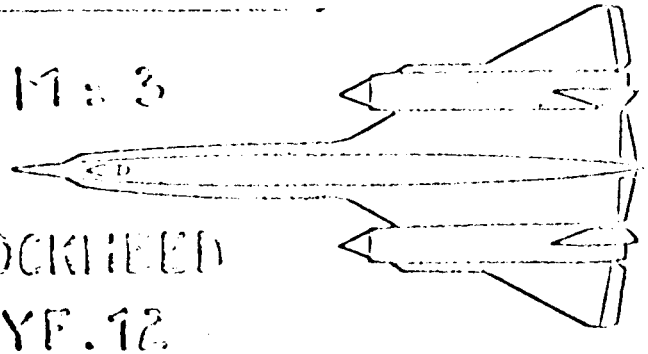

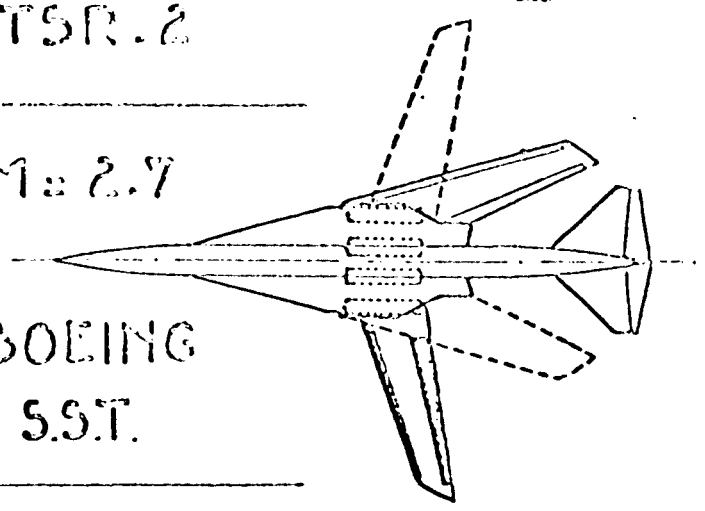

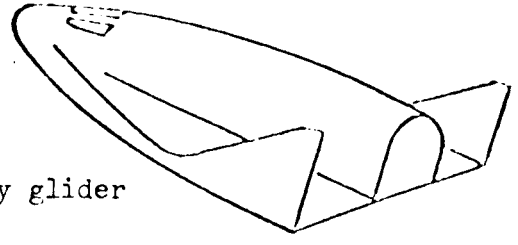

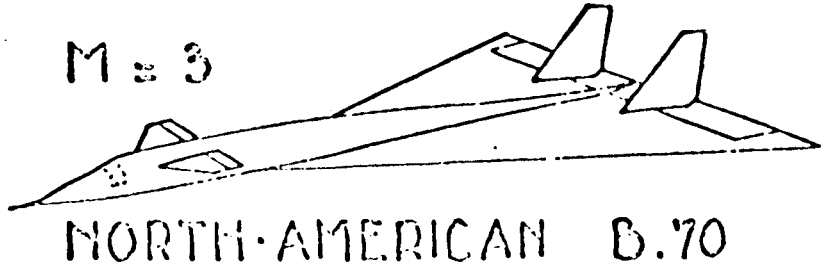

Fig.1 Slender Wings

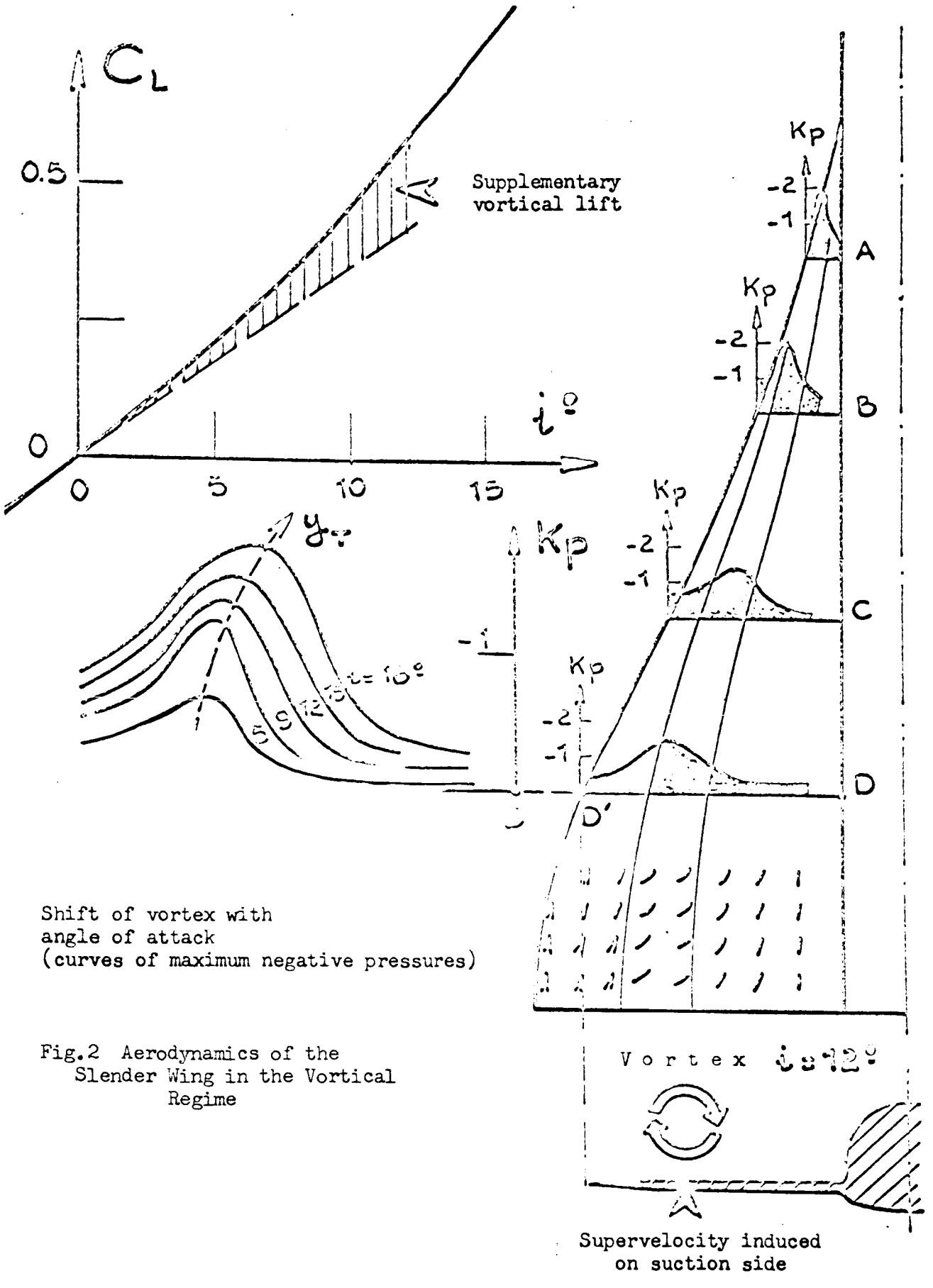

Shift of vortex with angle of attack (curves of maximum negative pressures)

Fig.2 Aerodynamics of the Slender Wing in the Vortical Regime

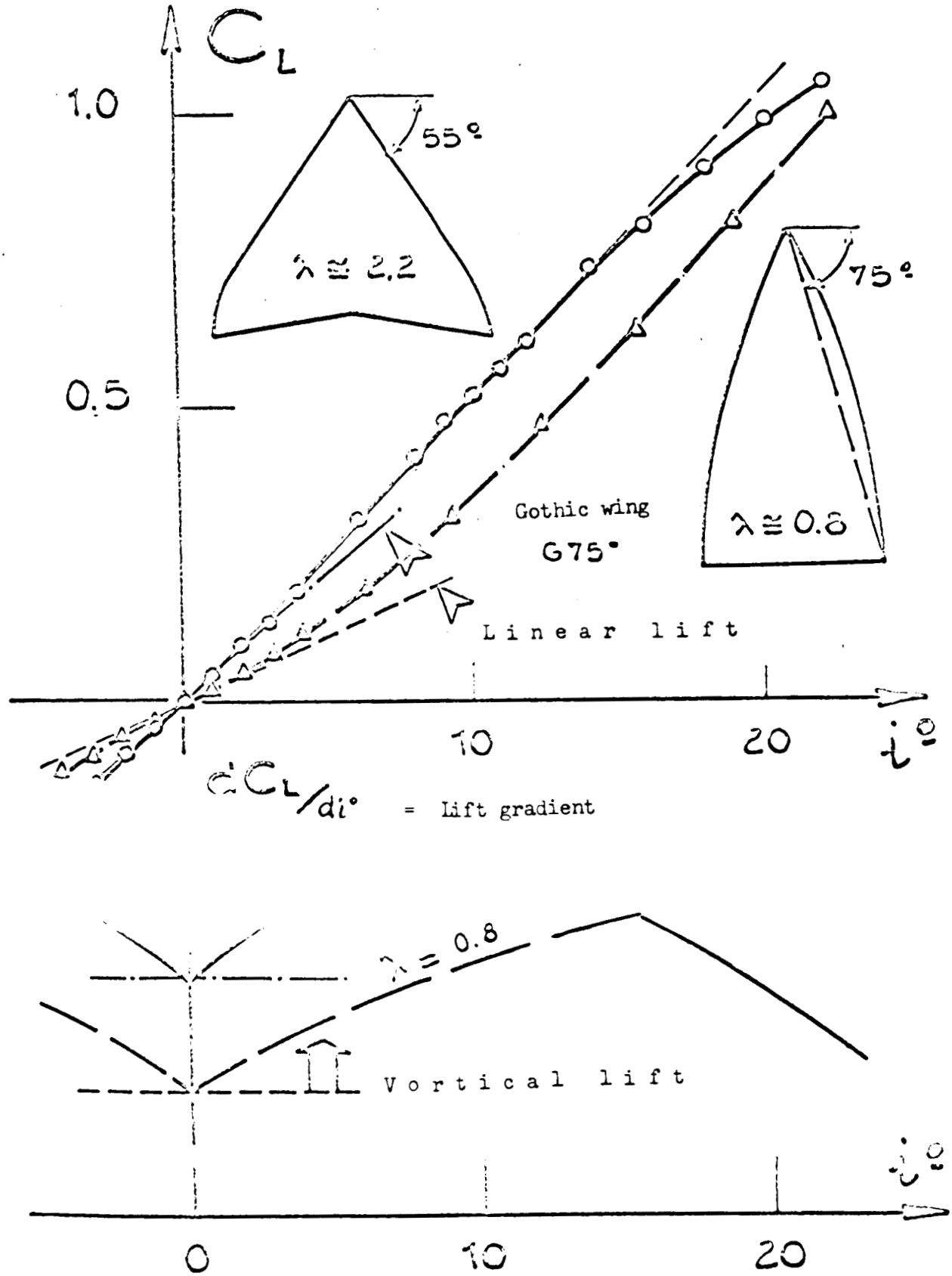

Fig.3 Plane Slender Wings with Sharp Leading Edge

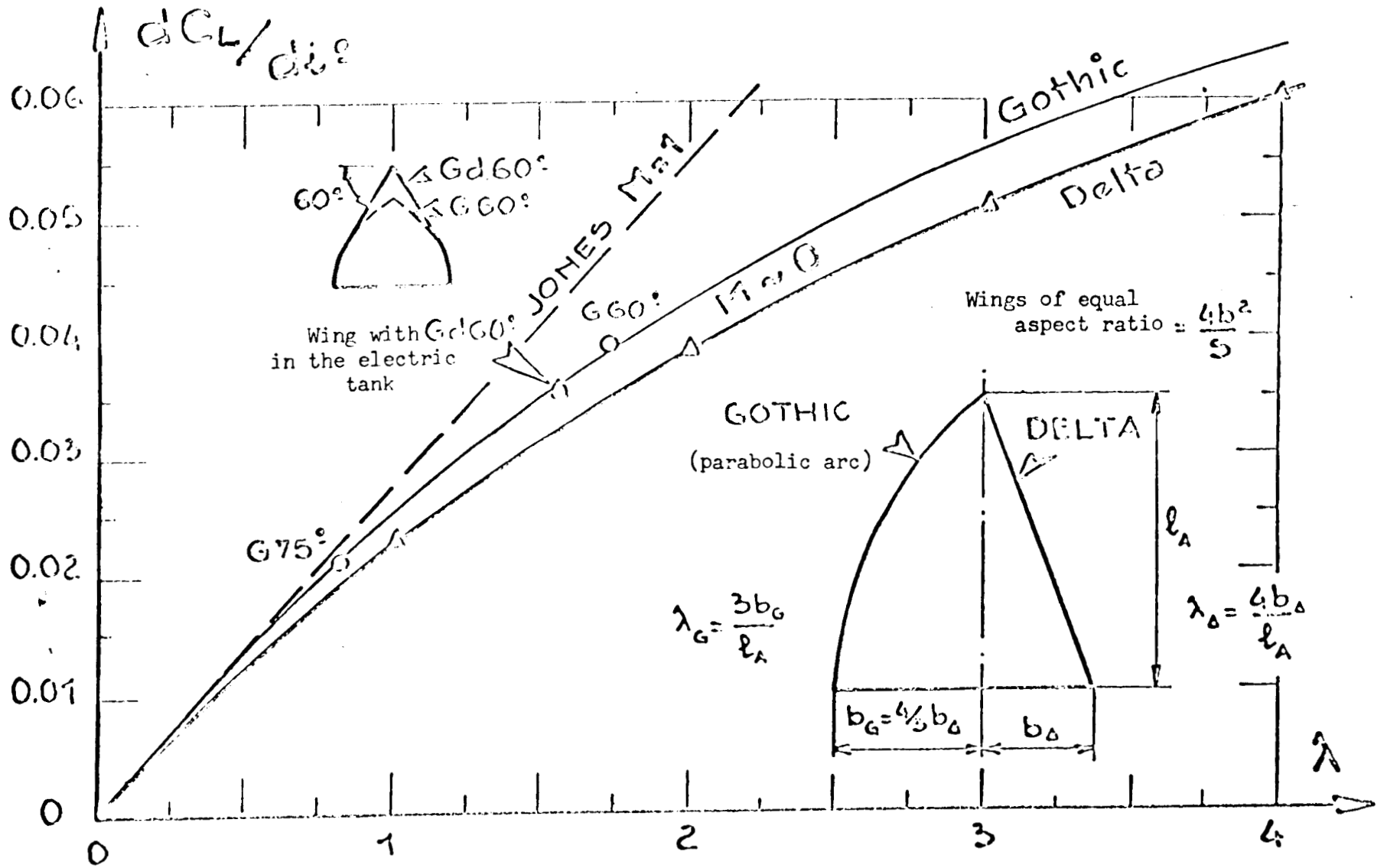

Fig.4 Calculation of the Linear Lift Gradient in Incompressible Flow (Theory of the Lifting Surface in the Rheoelectric Tank)

$$C_L = k R \left[\underbrace{\frac{\pi\lambda}{2} i_r}_{\text{Linear}} + \underbrace{\pi \lambda^{1/3} i^{5/3}}_{\text{Vortical}} \right] , \text{ with:}$$

$$R = \frac{C_{L\,(M=0)}}{C_{L\,(M=1)}} = \frac{4.9}{4.9+\lambda}$$ (Delta wings in the electric tank)

and k = Experimental coefficient, function of the wing geometry (thickness, etc.)

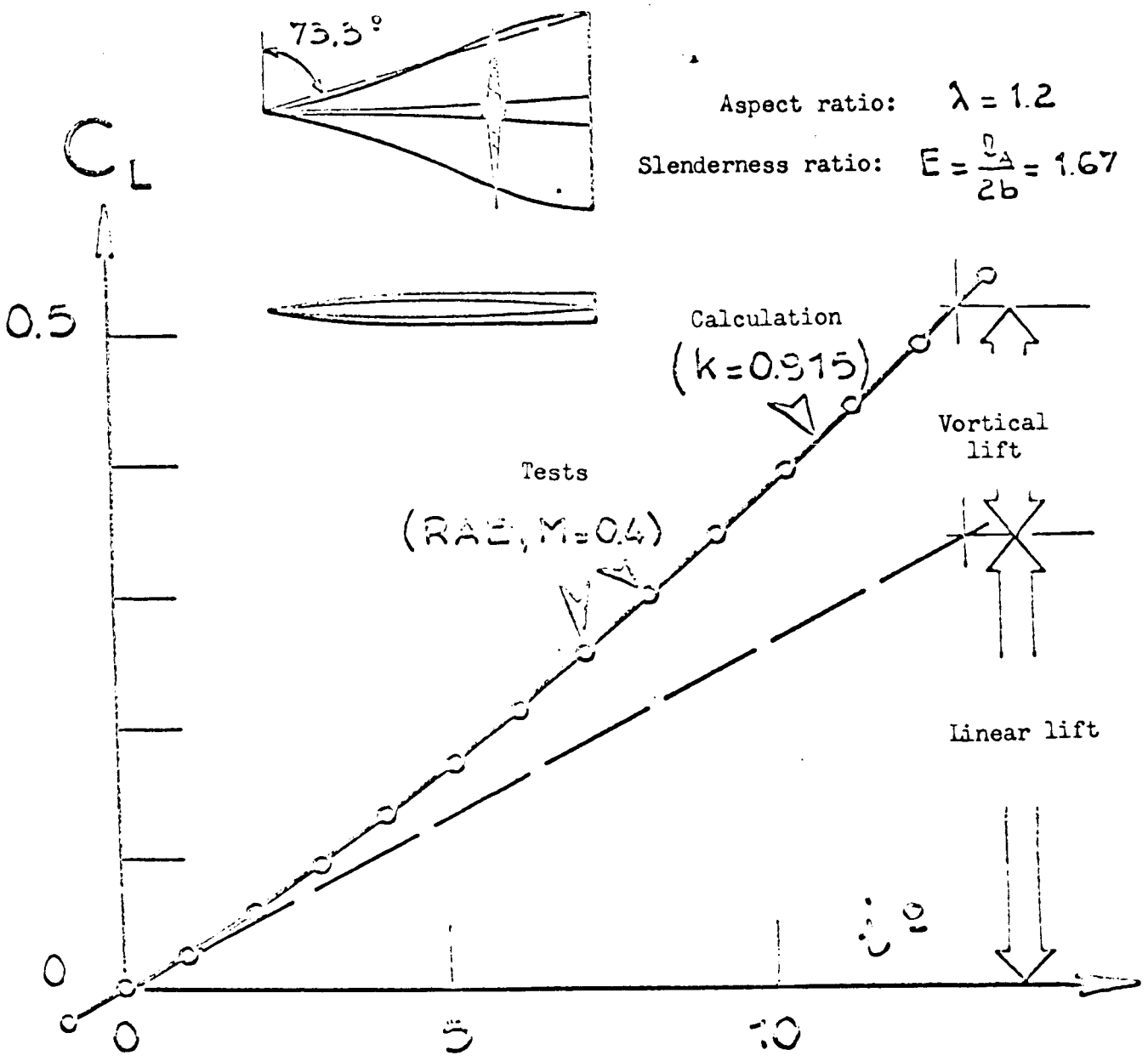

Fig.5 Lift of a Slender Wing

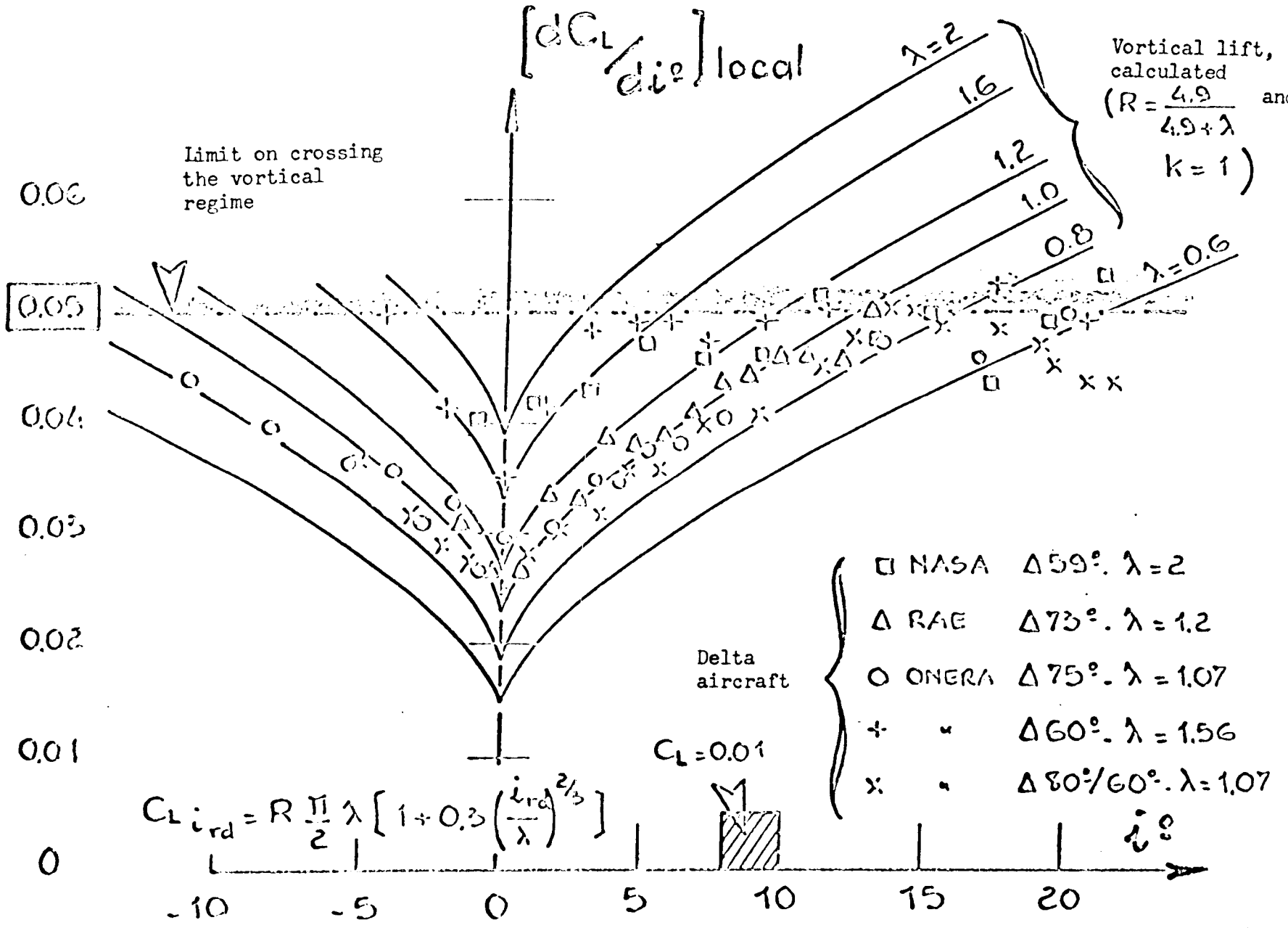
$\left[\frac{dC_L}{di^\circ}\right]$ local
Limit on crossing the vortical regime
Vortical lift, calculated ($R = \frac{4.9}{4.9+\lambda}$ and $k = 1$)
λ=2
1.6
1.2
1.0
0.8
λ=0.6
0.06
0.05
0.04
0.03
0.02
0.01
0
$C_L = 0.01$
Delta aircraft
□ NASA Δ59°. λ=2
Δ RAE Δ73°. λ=1.2
O ONERA Δ75°. λ=1.07
+ " Δ60°. λ=1.56
× " Δ80°/60°. λ=1.07
$C_{L\,i_{rd}} = R\frac{\pi}{2}\lambda\left[1+0.3\left(\frac{i_{rd}}{\lambda}\right)^{2/3}\right]$
i°
-10
-5
0
5
10
15
20

Fig.6

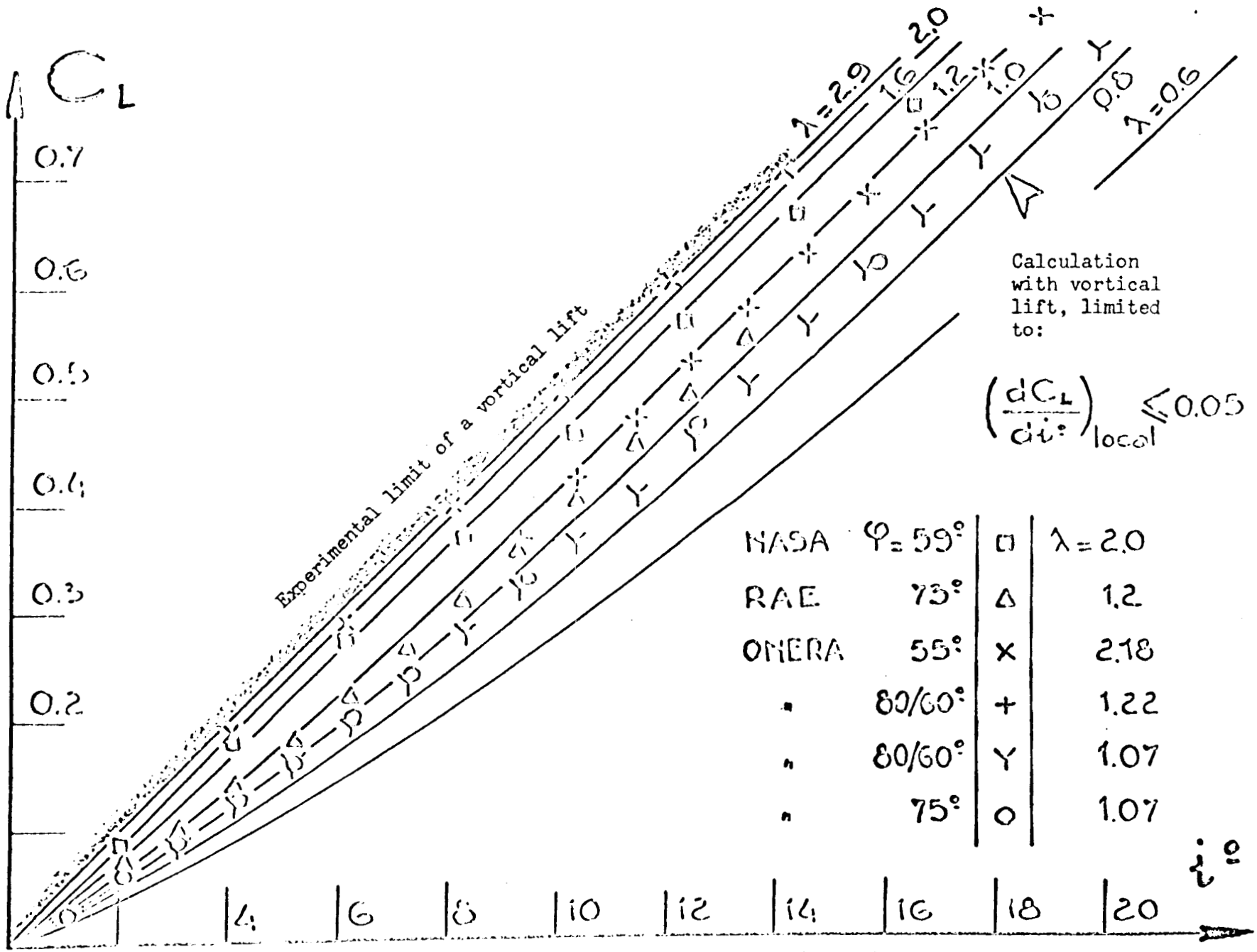

Fig.7 Tests on Sharp-Edged Delta Aircraft

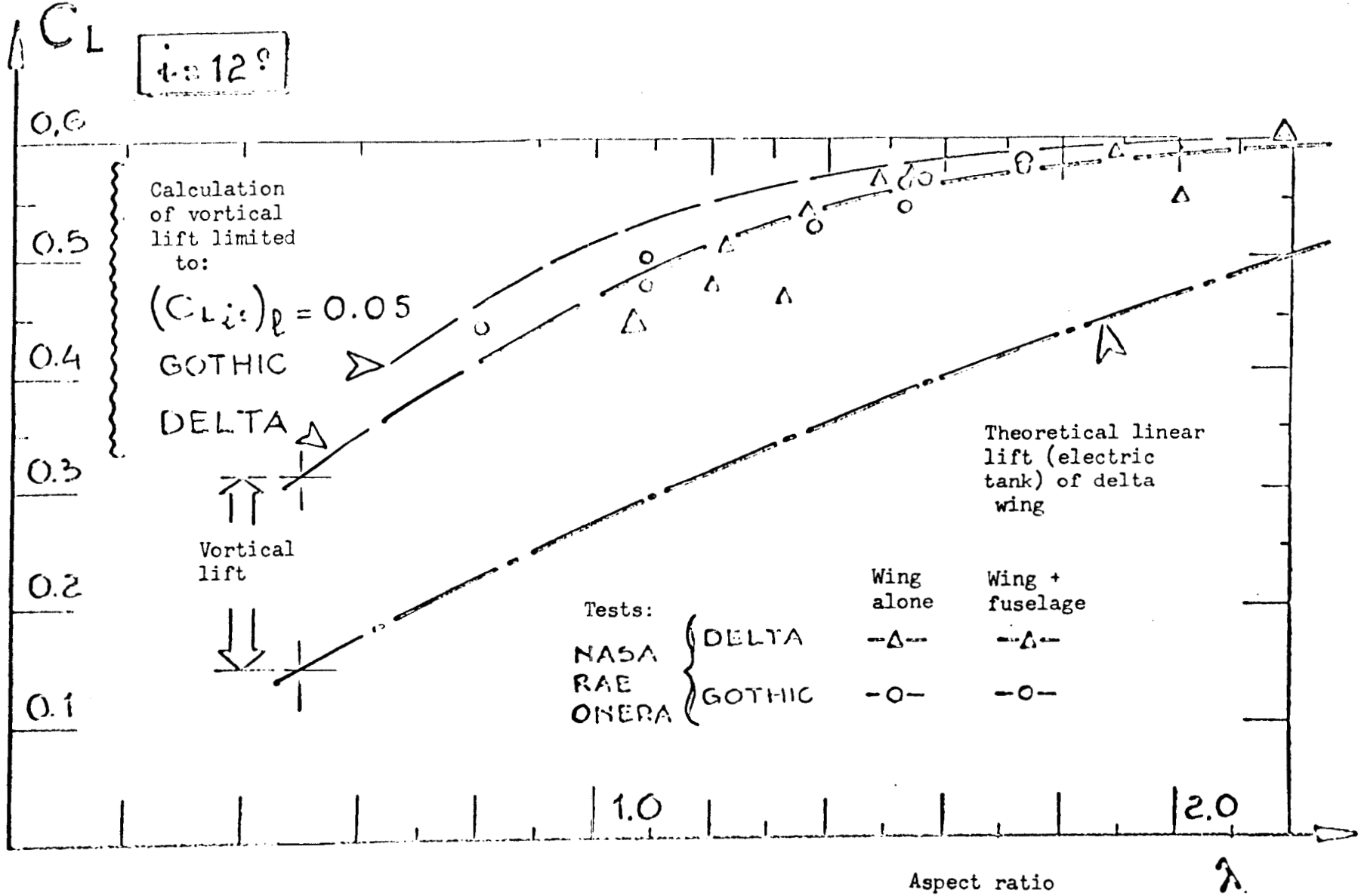

Fig.8 Experimental Lift on Approach; Aircraft with Slender Wings (Uncompensated) and Sharp Leading Edge

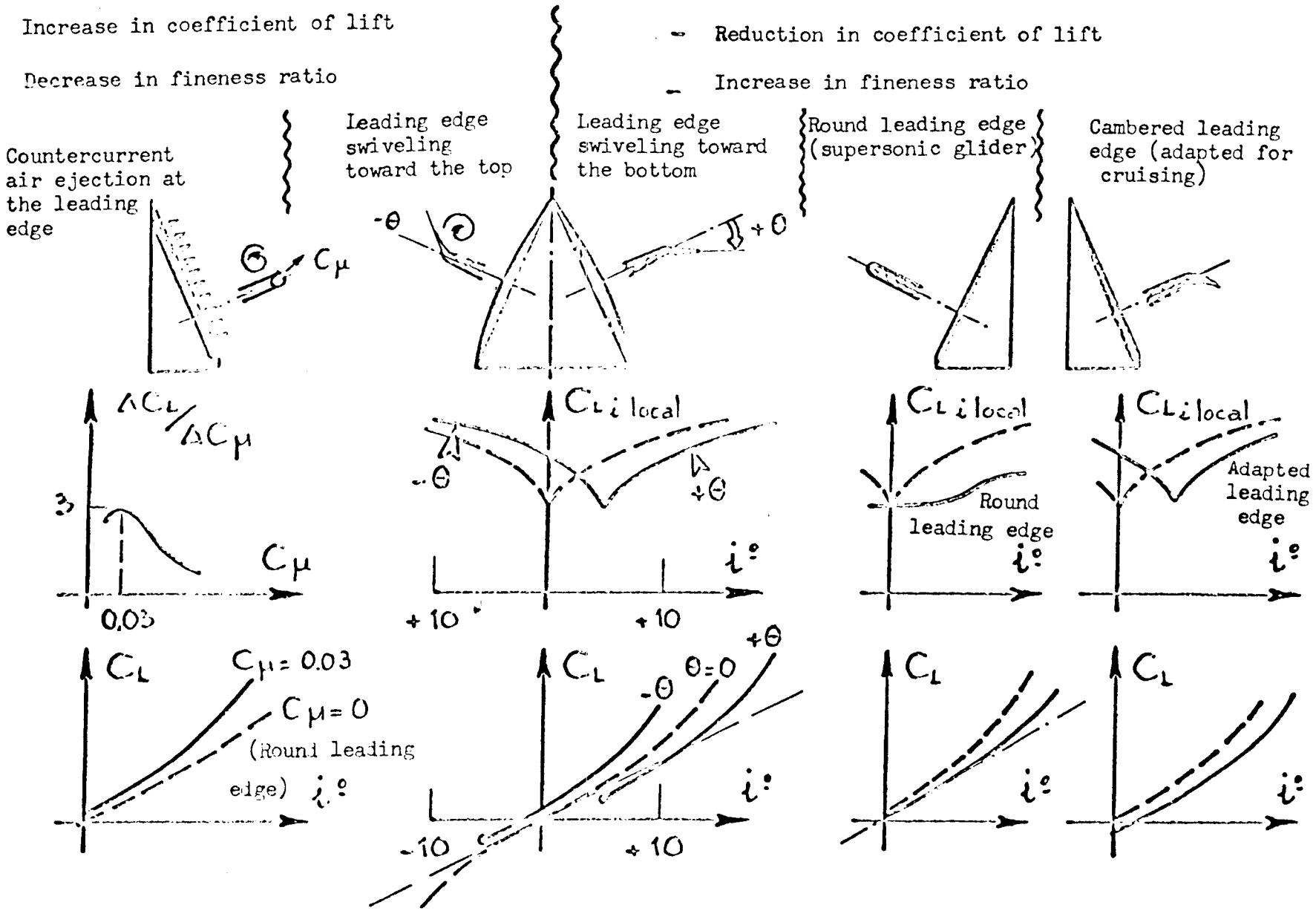

Fig.9 Influence on the Vortical Lift

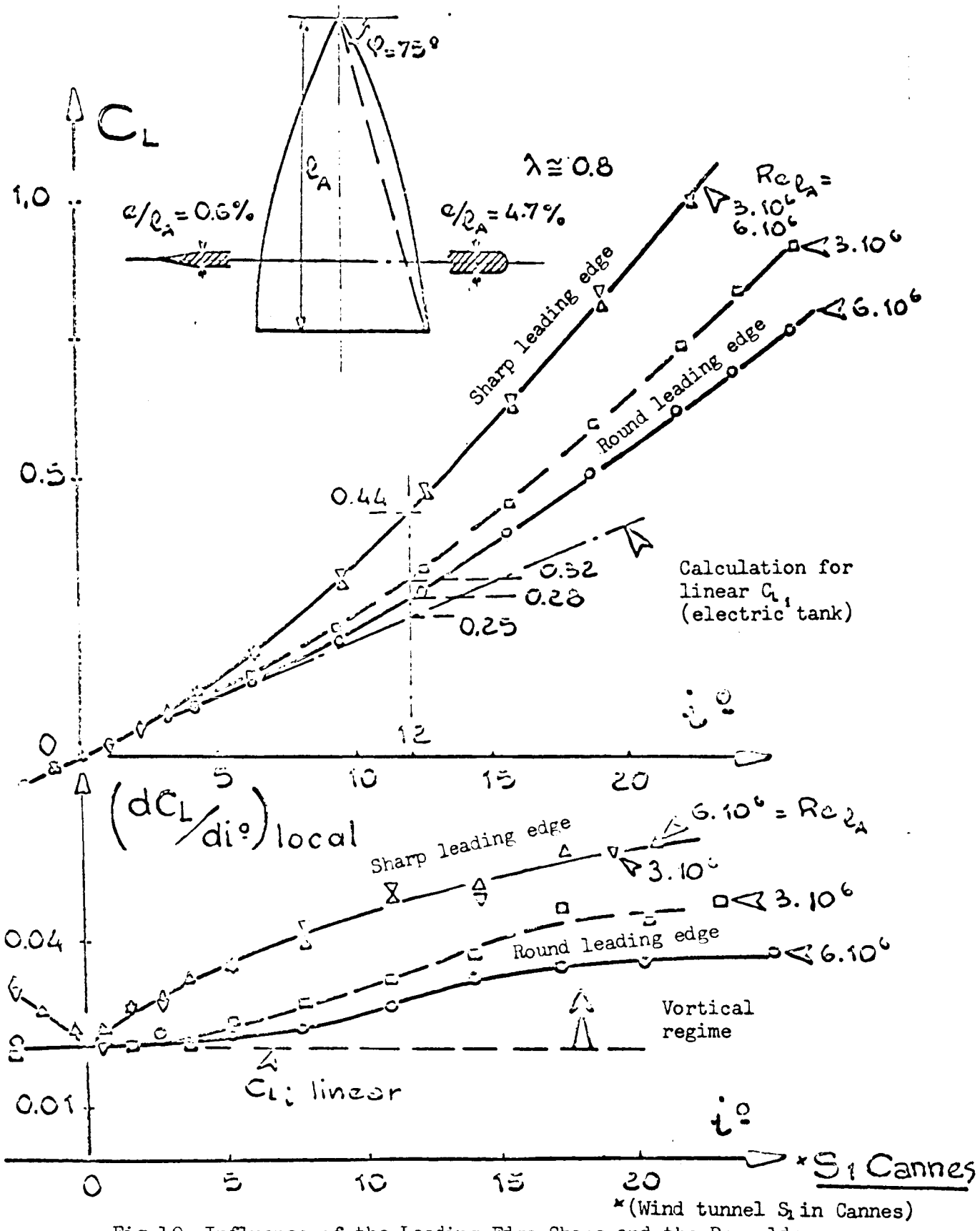

Fig.10 Influence of the Leading-Edge Shape and the Reynolds Number on the Lift of a Slender Wing; Plane Gothic Wing G = 75°

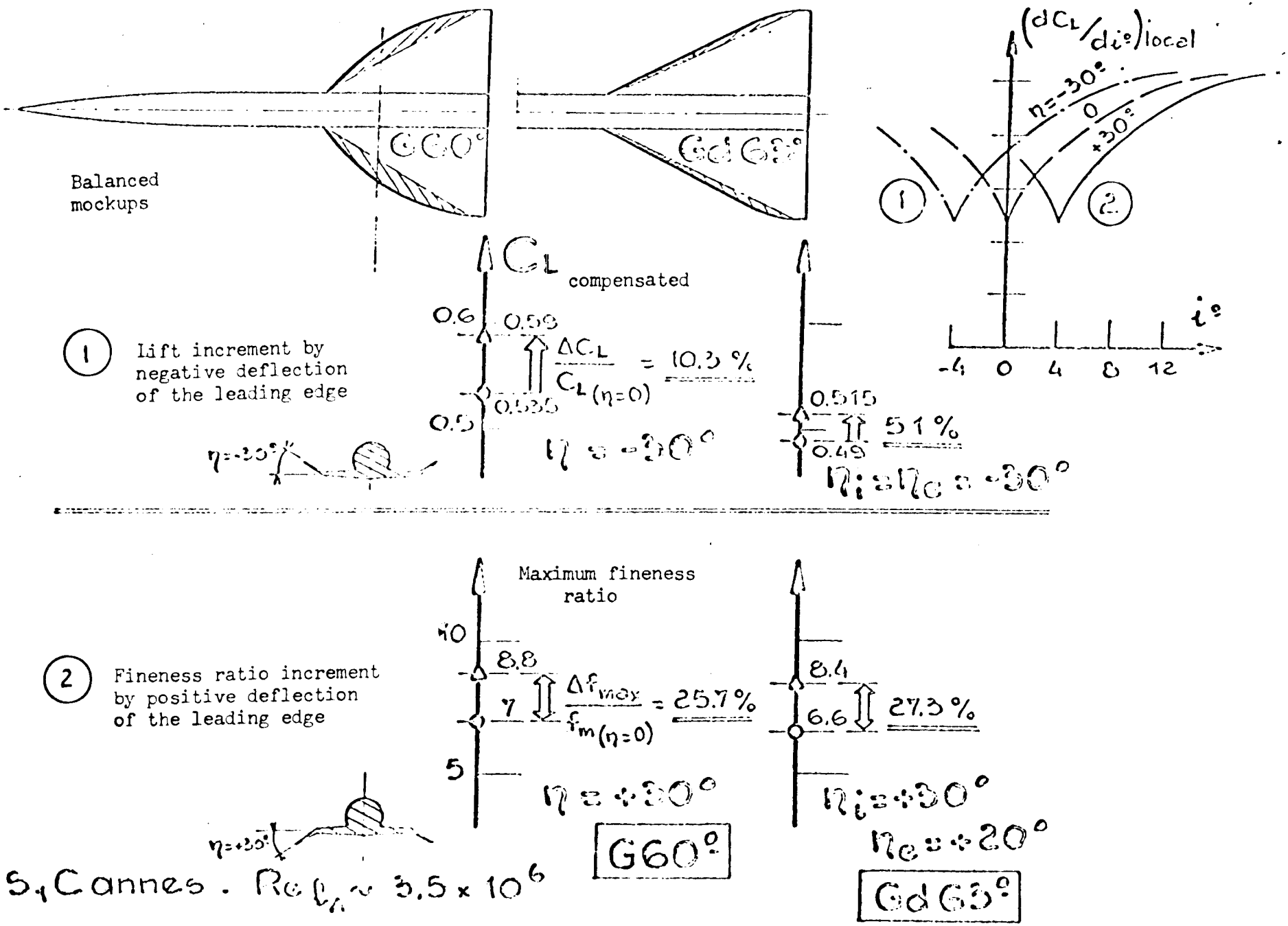

Fig.11 Swivelable Leading Edge on Slender Wings

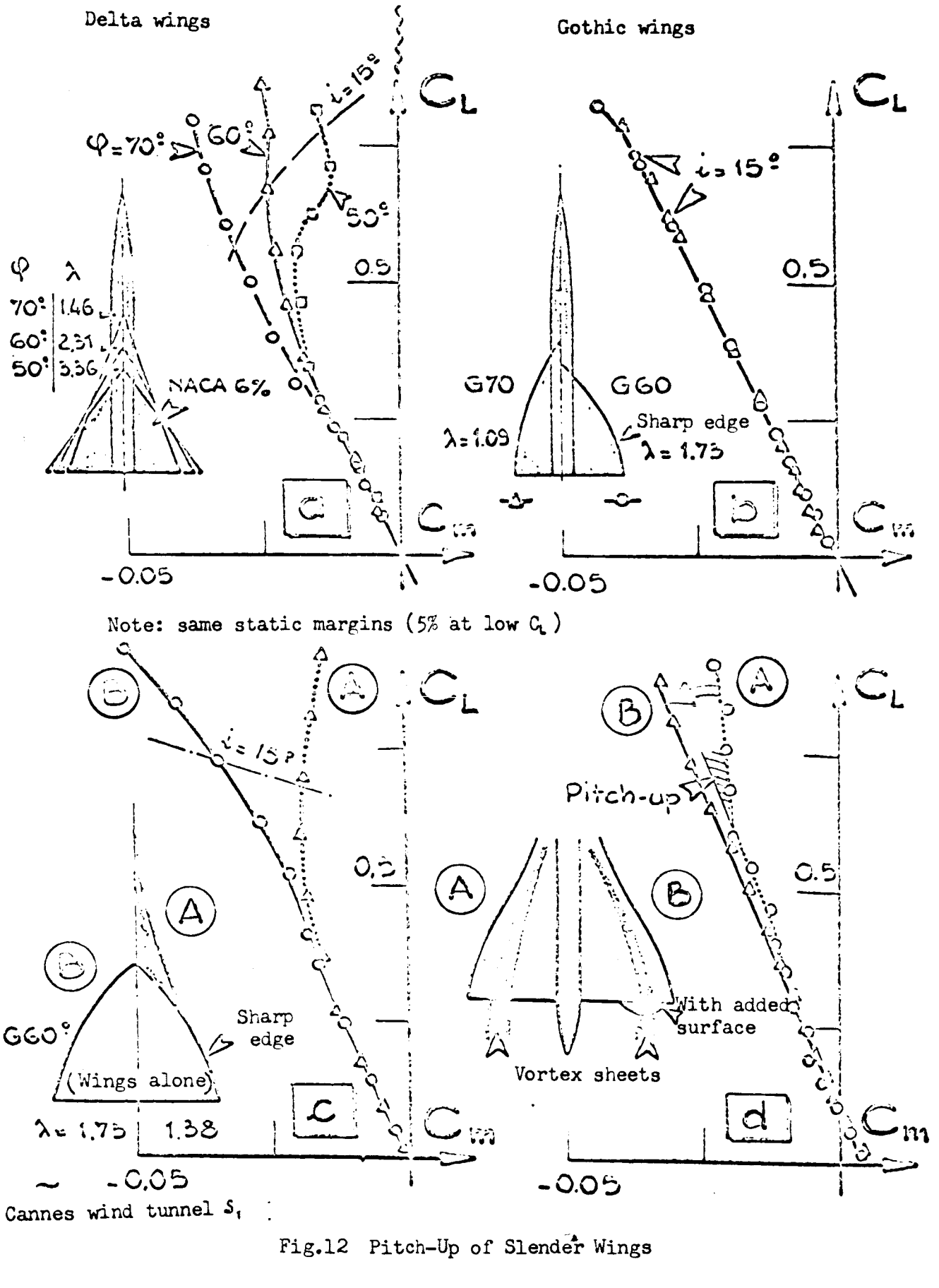

Fig.12 Pitch-Up of Slender Wings

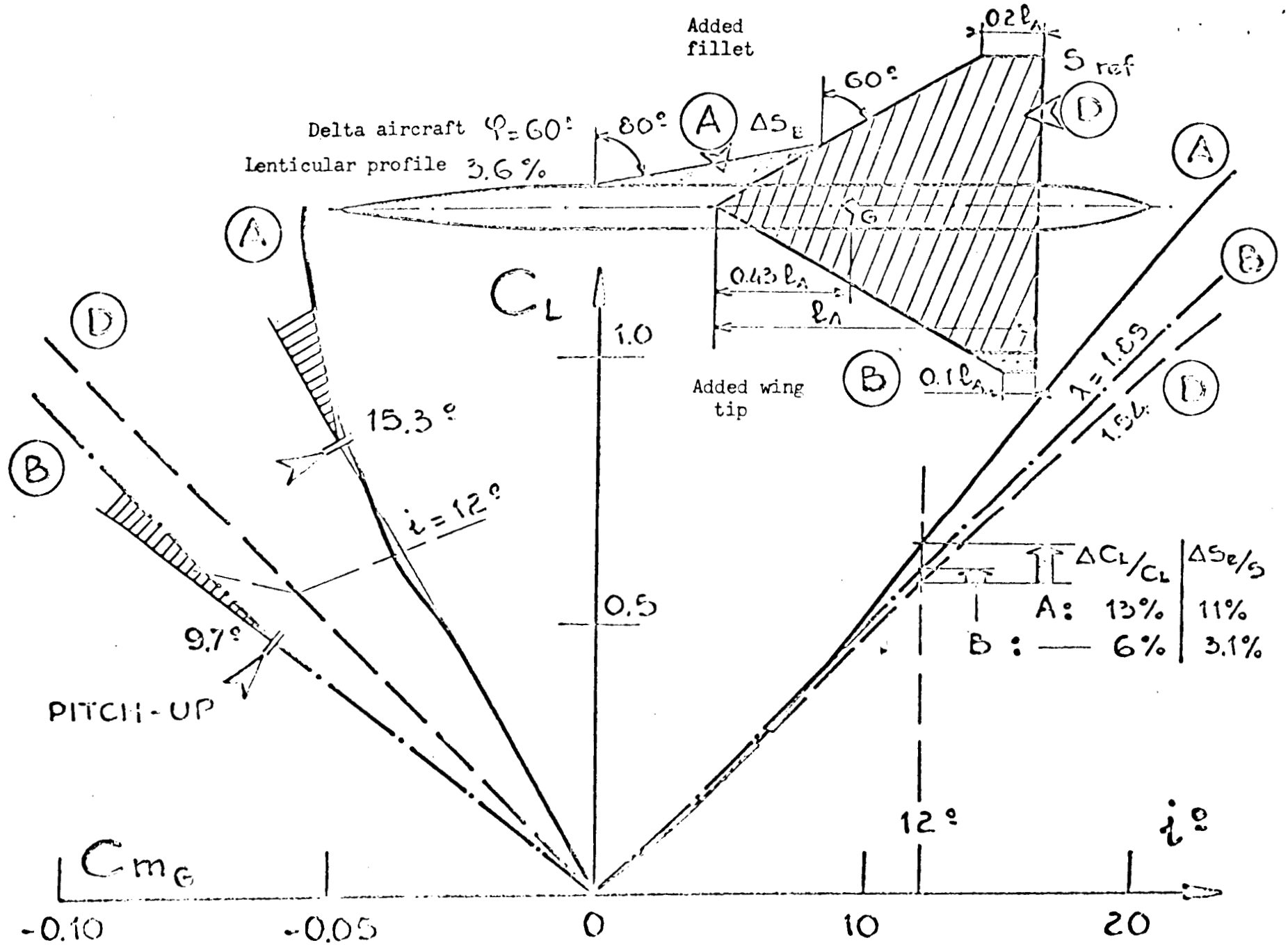

Fig.13 Influence of an Added Fillet or Wing Tip

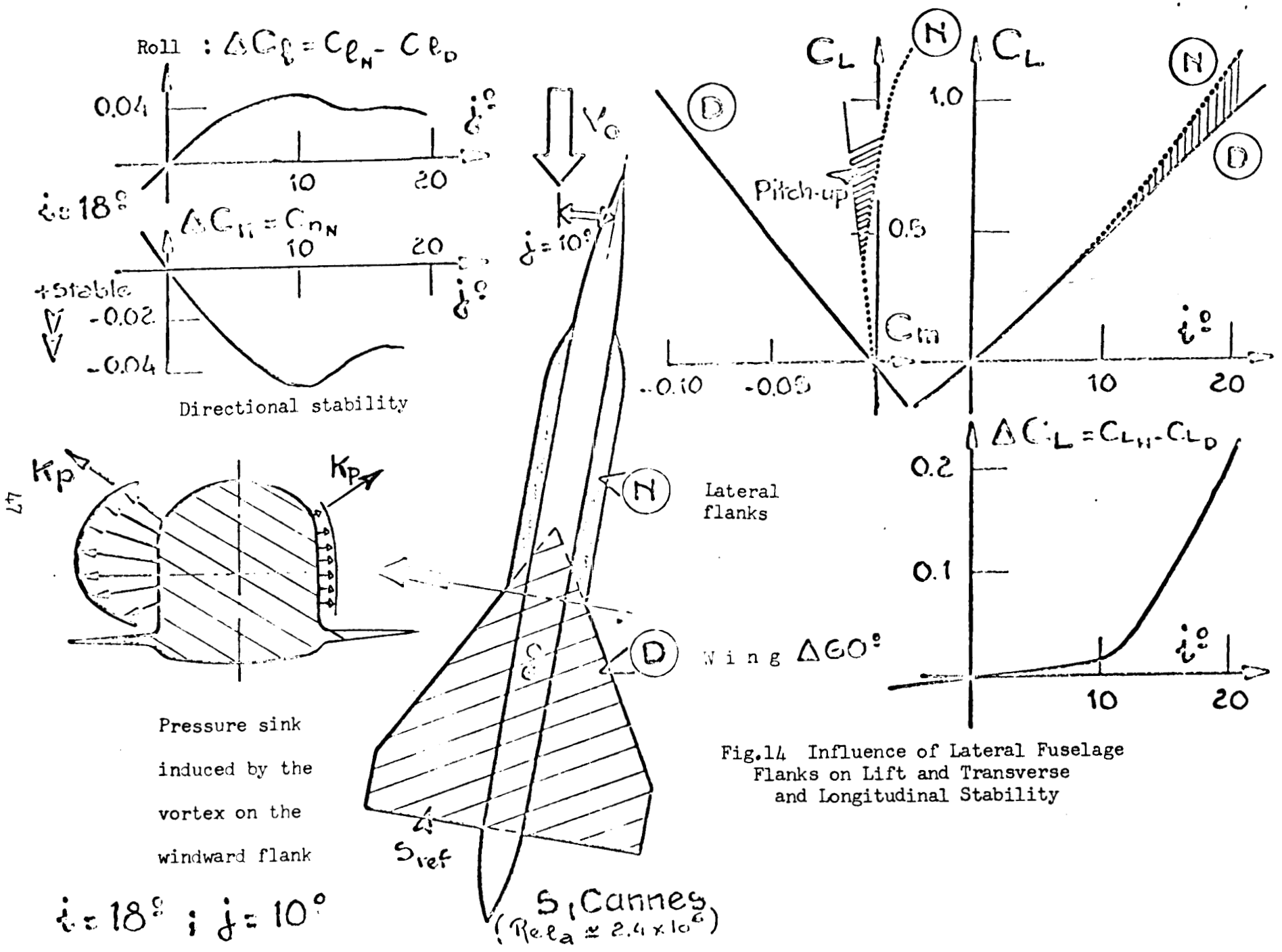

Fig.14 Influence of Lateral Fuselage Flanks on Lift and Transverse and Longitudinal Stability

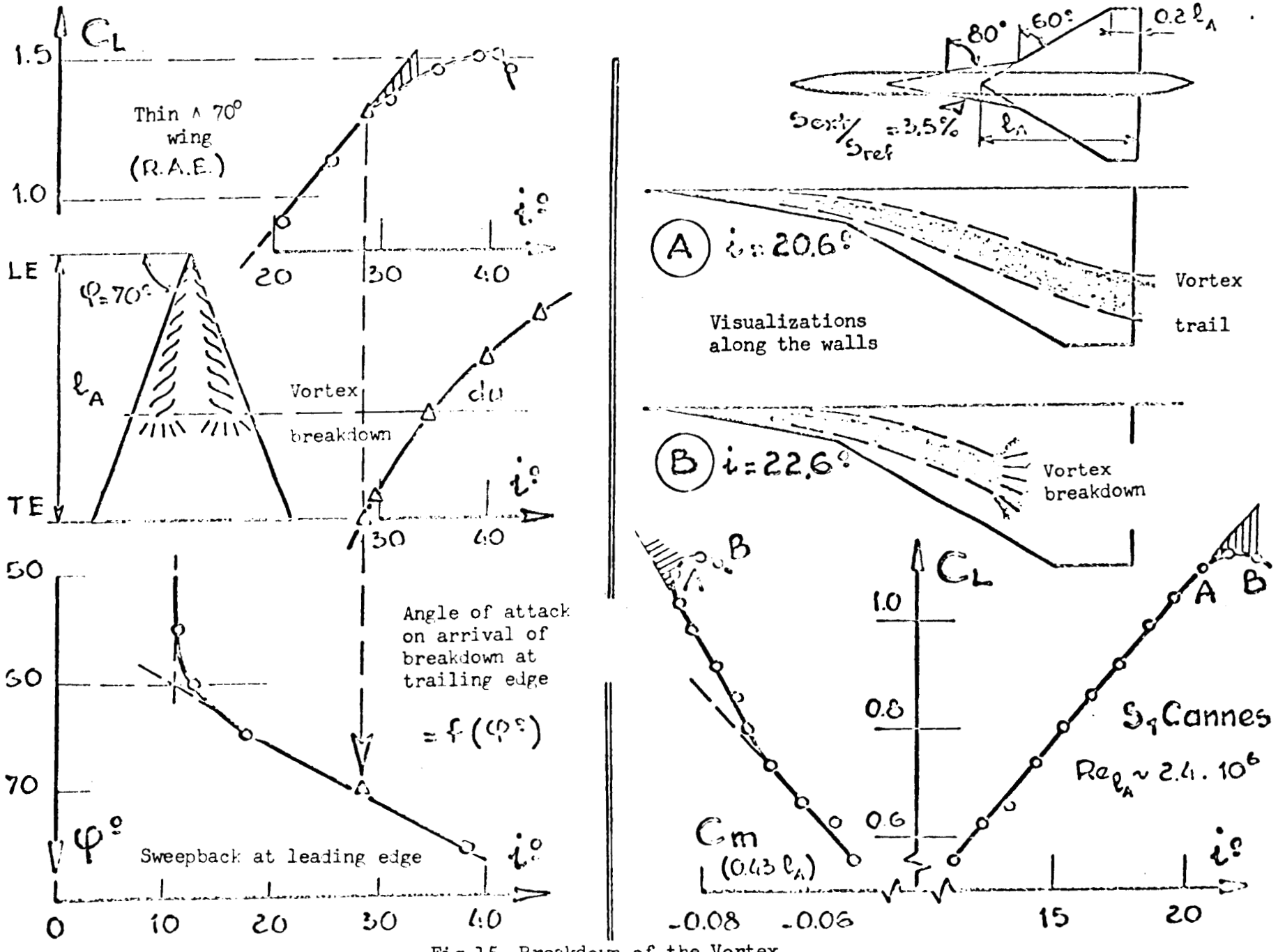

Fig.15 Breakdown of the Vortex

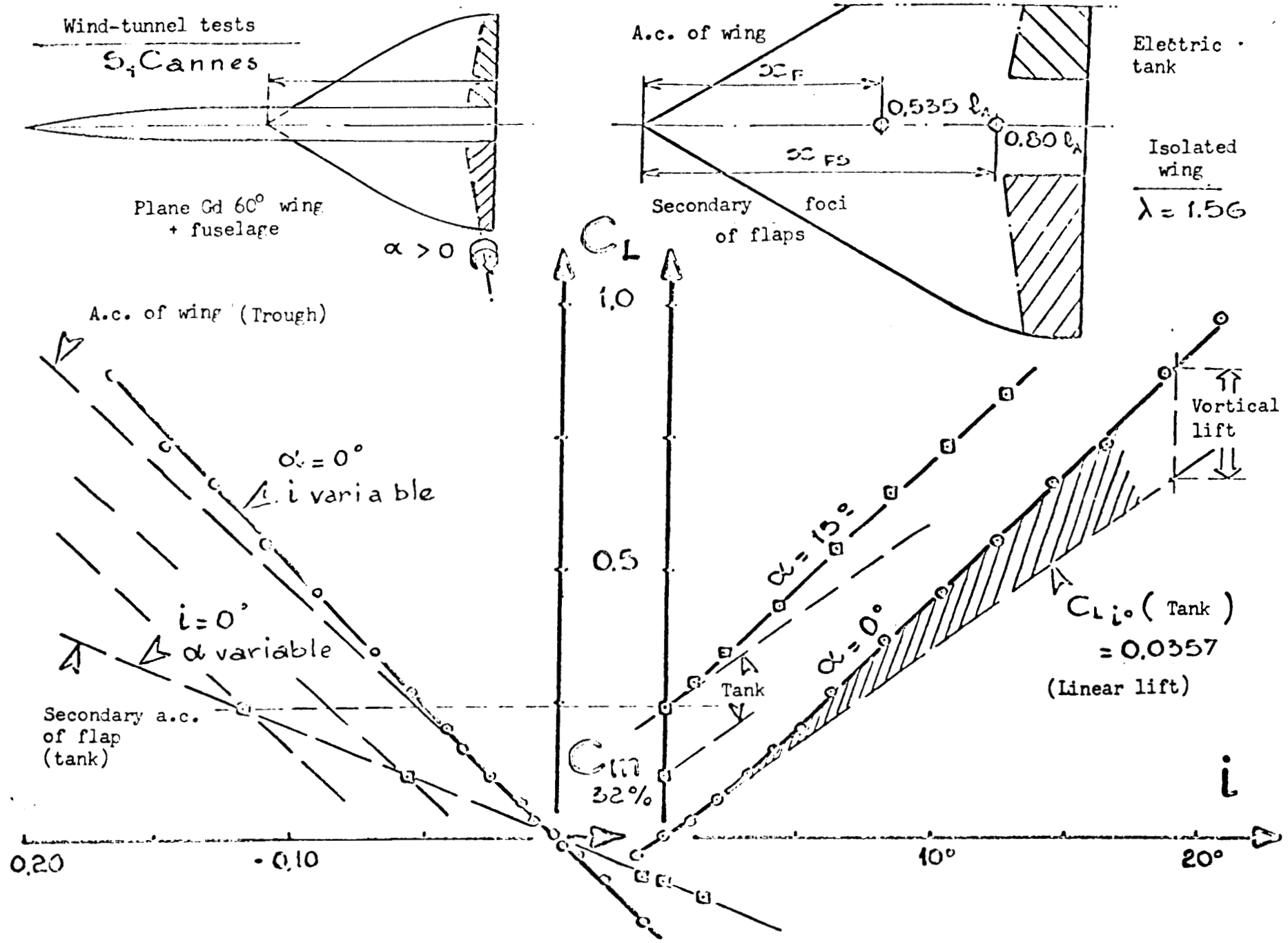
Wind-tunnel tests
S. Cannes
Plane Gd 60° wing
+ fuselage
α > 0
A.c. of wing
Electric tank
0.535 ℓA
0.80 ℓA
Isolated wing
λ = 1.56
Secondary foci of flaps
CL
1.0
0.5
A.c. of wing (Trough)
α = 0°
i variable
i = 0°
α variable
Secondary a.c. of flap (tank)
Tank
Cm 32%
Vortical lift
α = 15°
α = 0°
CL i° (Tank) = 0.0357
(Linear lift)
i
0.20
- 0.10
10°
20°

Fig.16

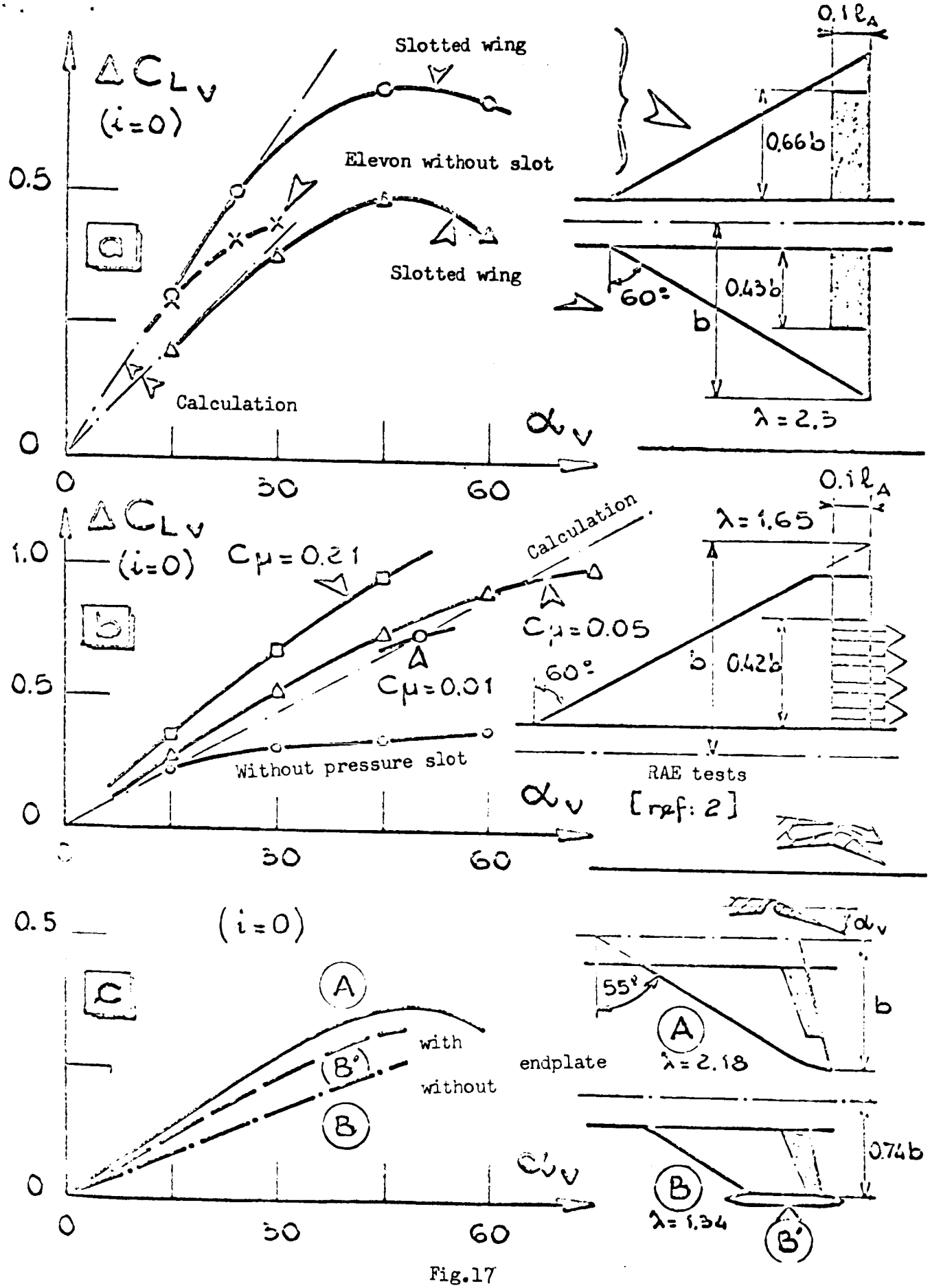
Slotted wing
Elevon without slot
Slotted wing
Calculation
0.5
0
0
30
60
(i=0)
a
0.1 l_A
0.66b
60°
0.43b
b
λ = 2.3
1.0
0.5
(i=0)
Cμ = 0.21
Cμ = 0.05
Cμ = 0.01
Calculation
Without pressure slot
b
0.42b
60°
λ = 1.65
RAE tests
[ref: 2]
0.5
(i=0)
C
A
B'
B
with
without
endplate
55°
λ = 2.18
λ = 1.34
0.74b

Fig.17

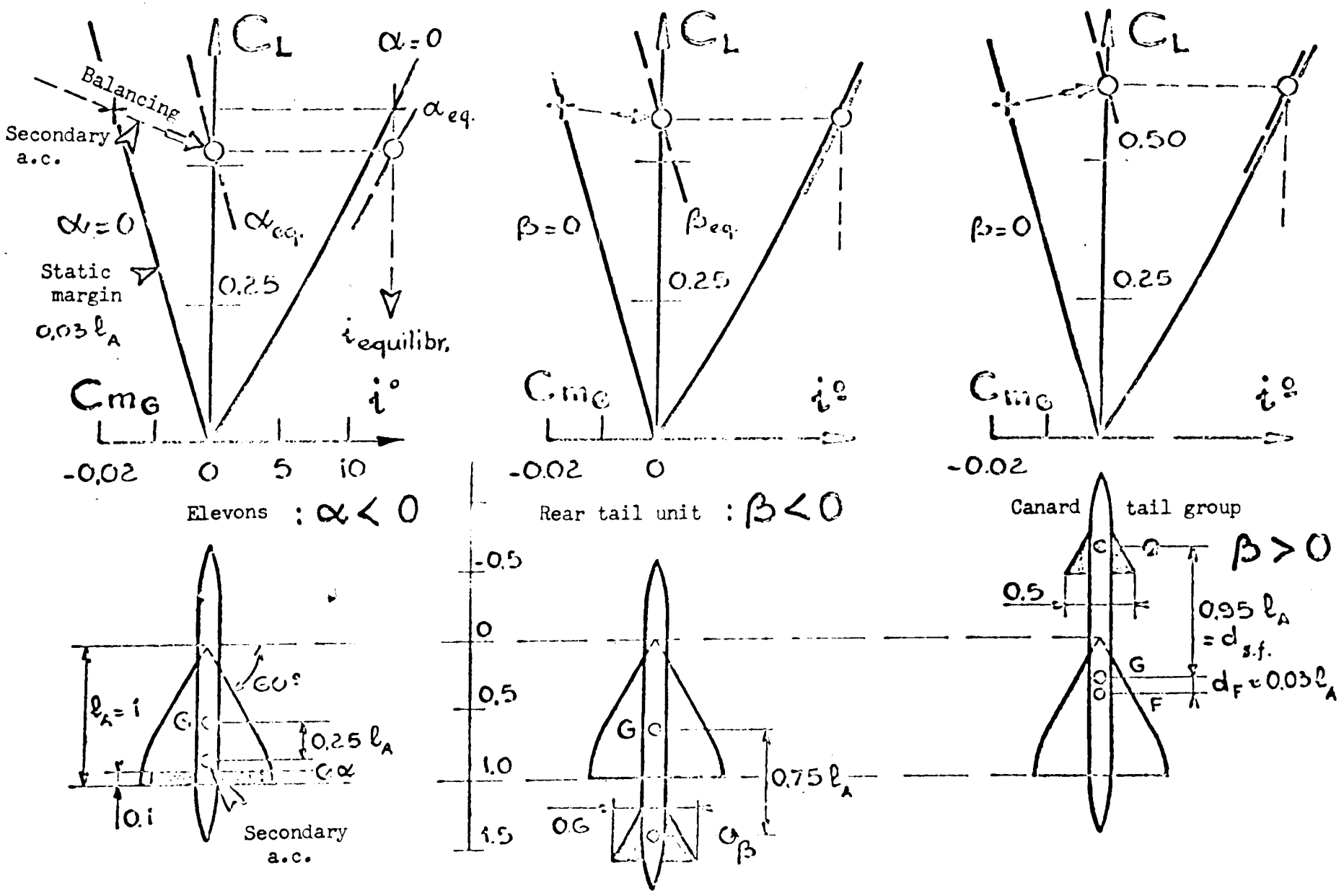

Fig.18 Principle of Longitudinal Balancing

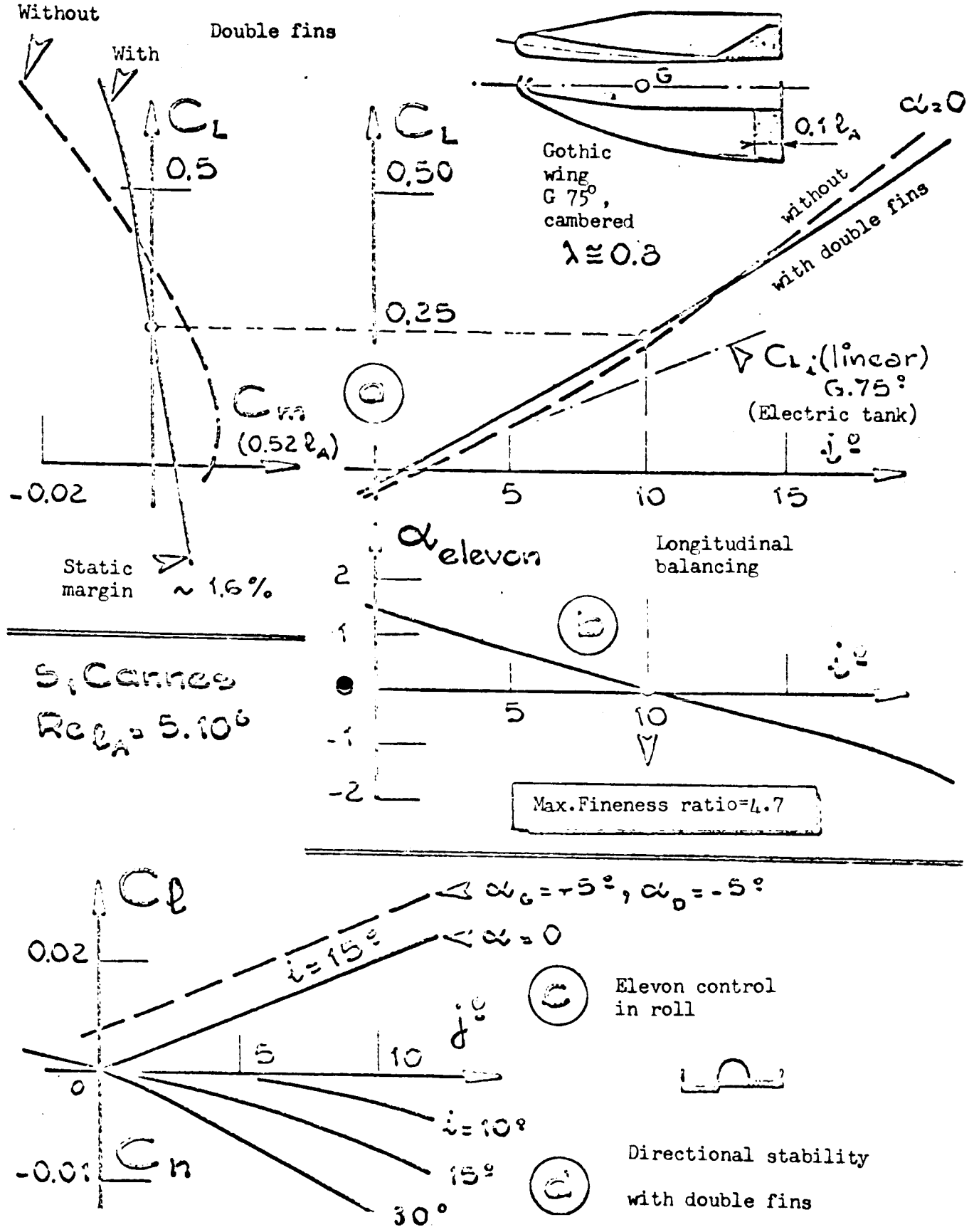

Fig.19 Supersonic Glider on Landing

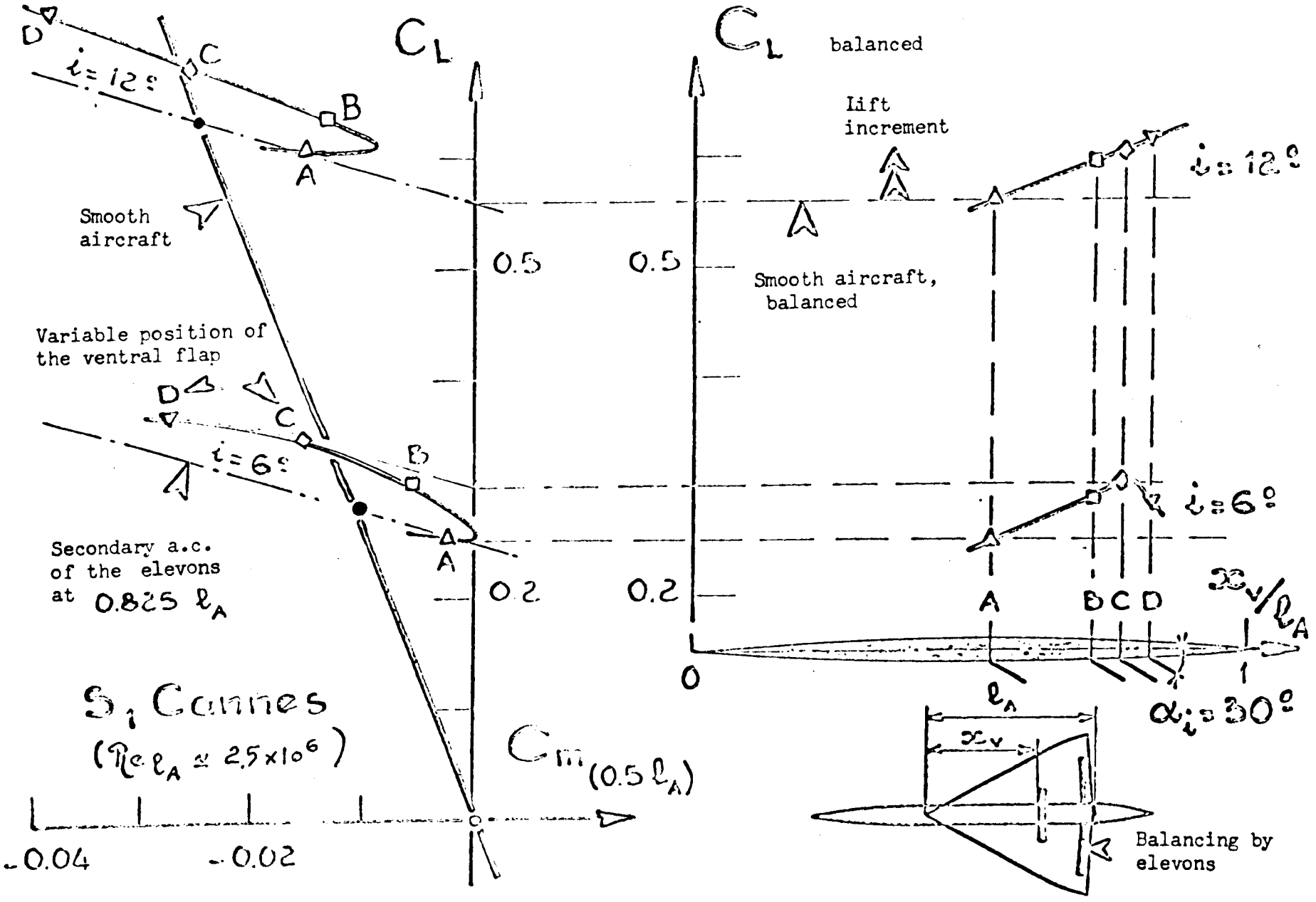

Fig.20 Hyperlift by Ventral Pressure-Side Flap

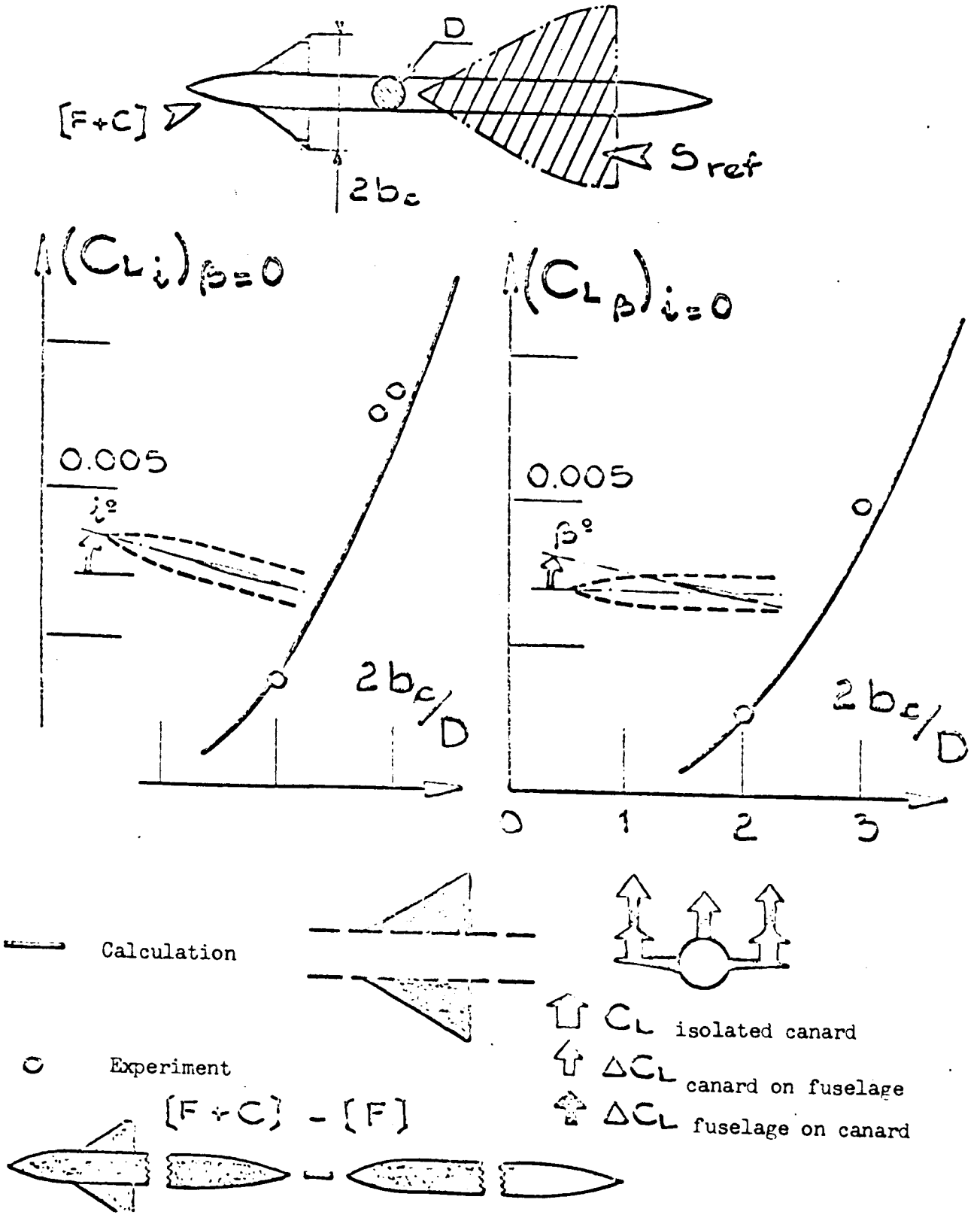

Fig.21 Lift Gradient of a Canard Control Surface in the Presence of a Fuselage

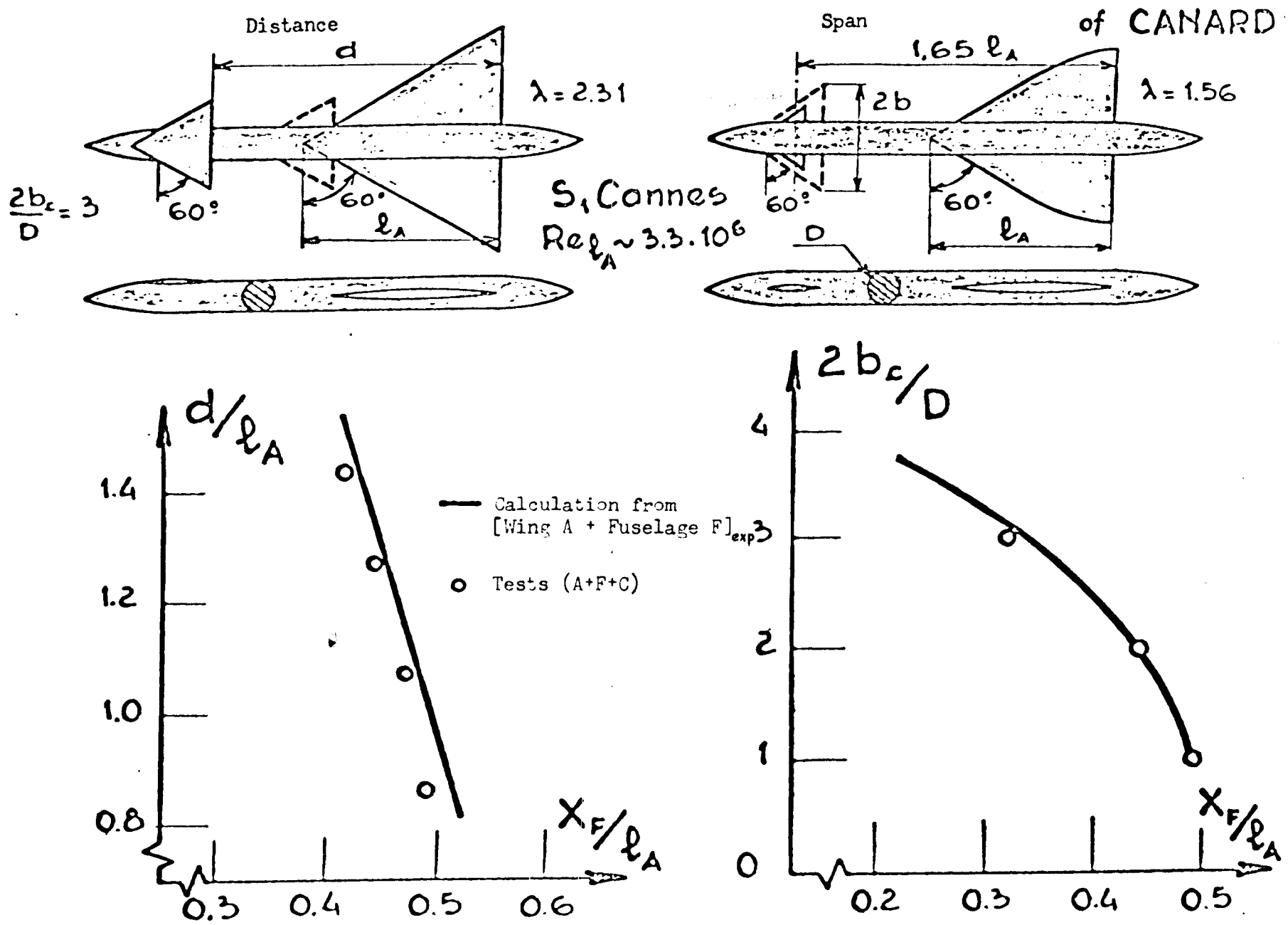

Fig.22 Variation in Position of the Aerodynamic Center as a Function of Distance and Span of the Canard

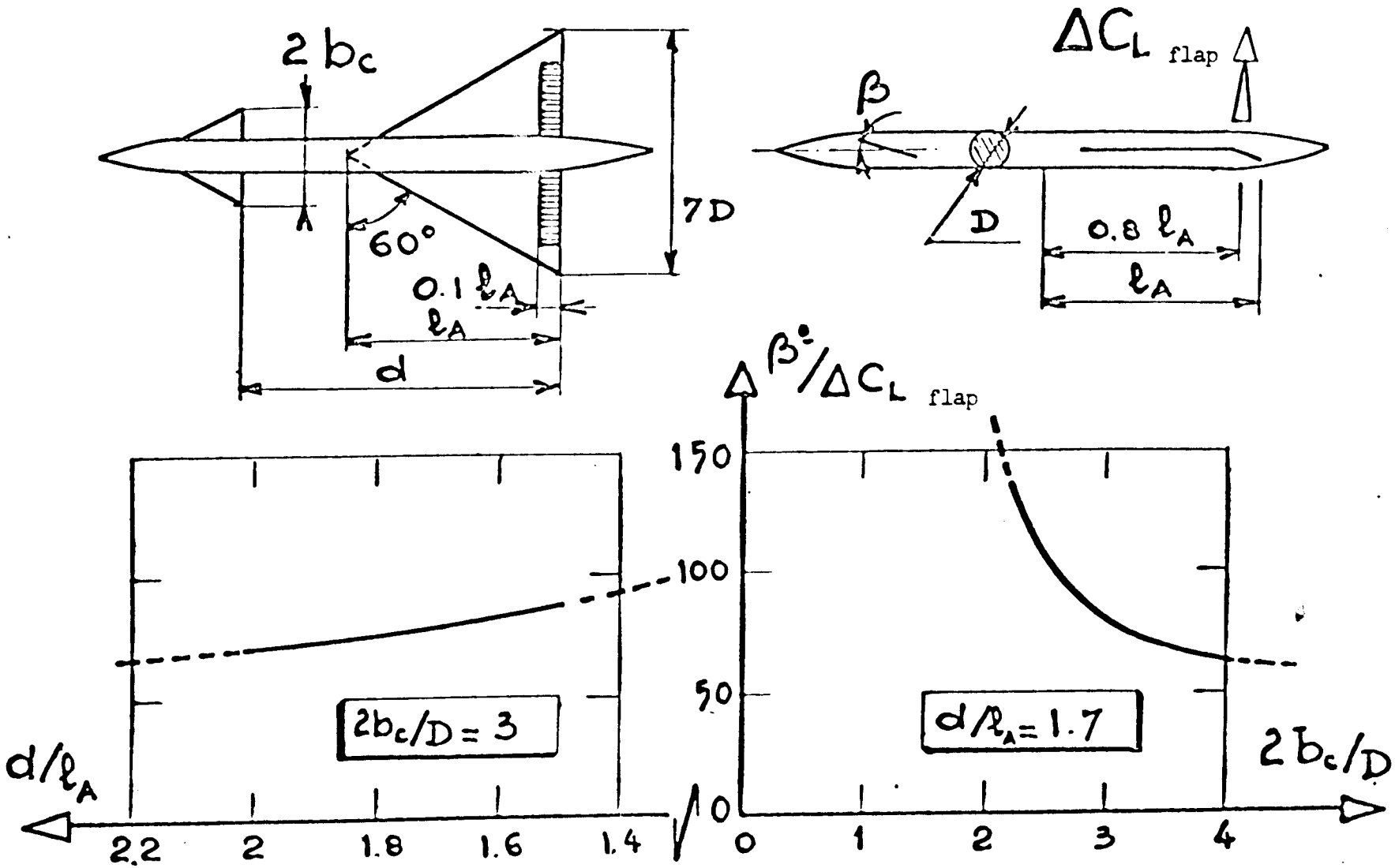

Fig.23 Calculation of the Deflection of a Canard Control Surface for Balancing of a Hyperlift Flap
(Static Margin: 0.05 l_A)

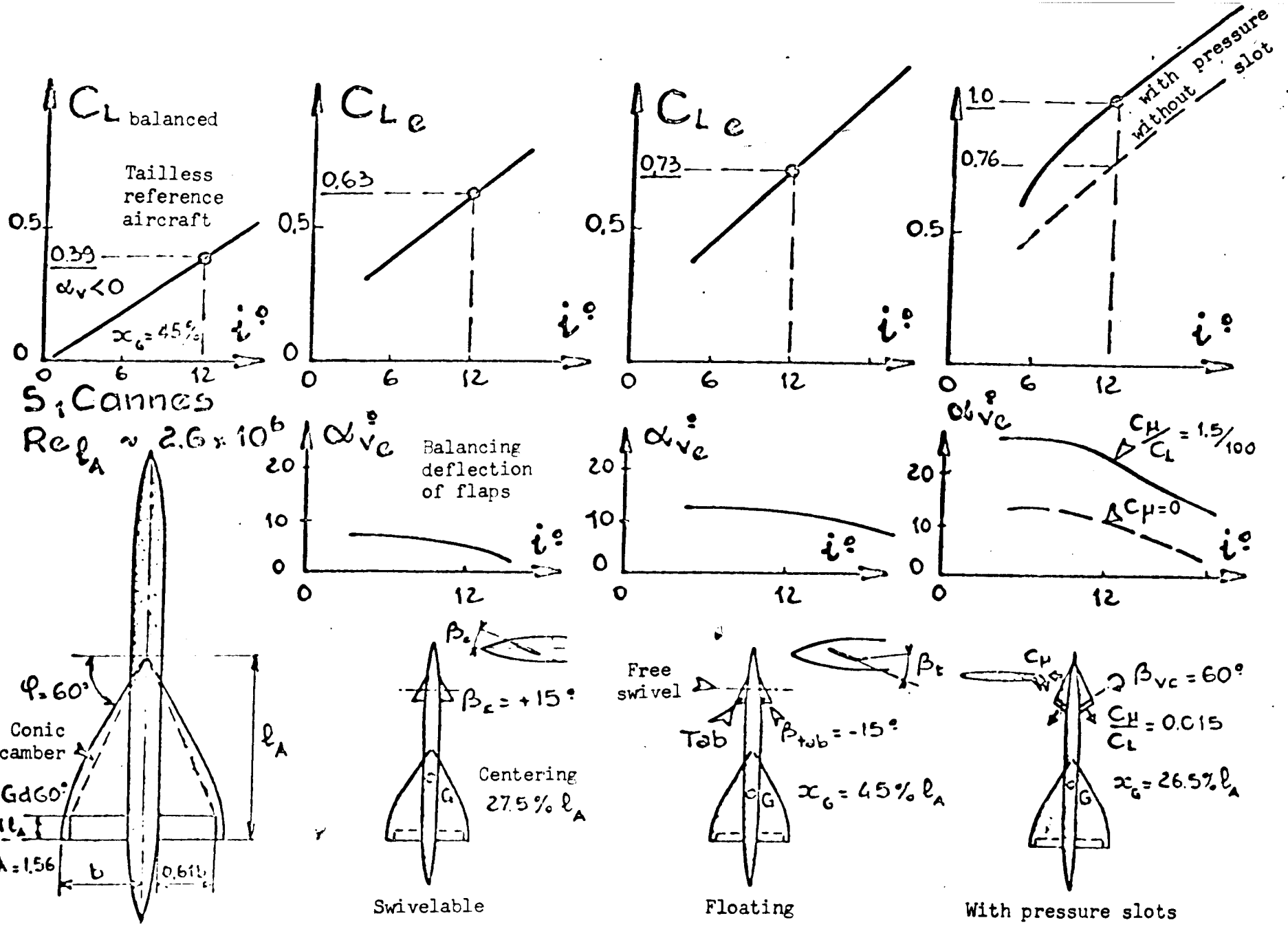

Fig.24 Balanced Lifts of Canard Aircraft
(Same Static Margin, 4.3%)

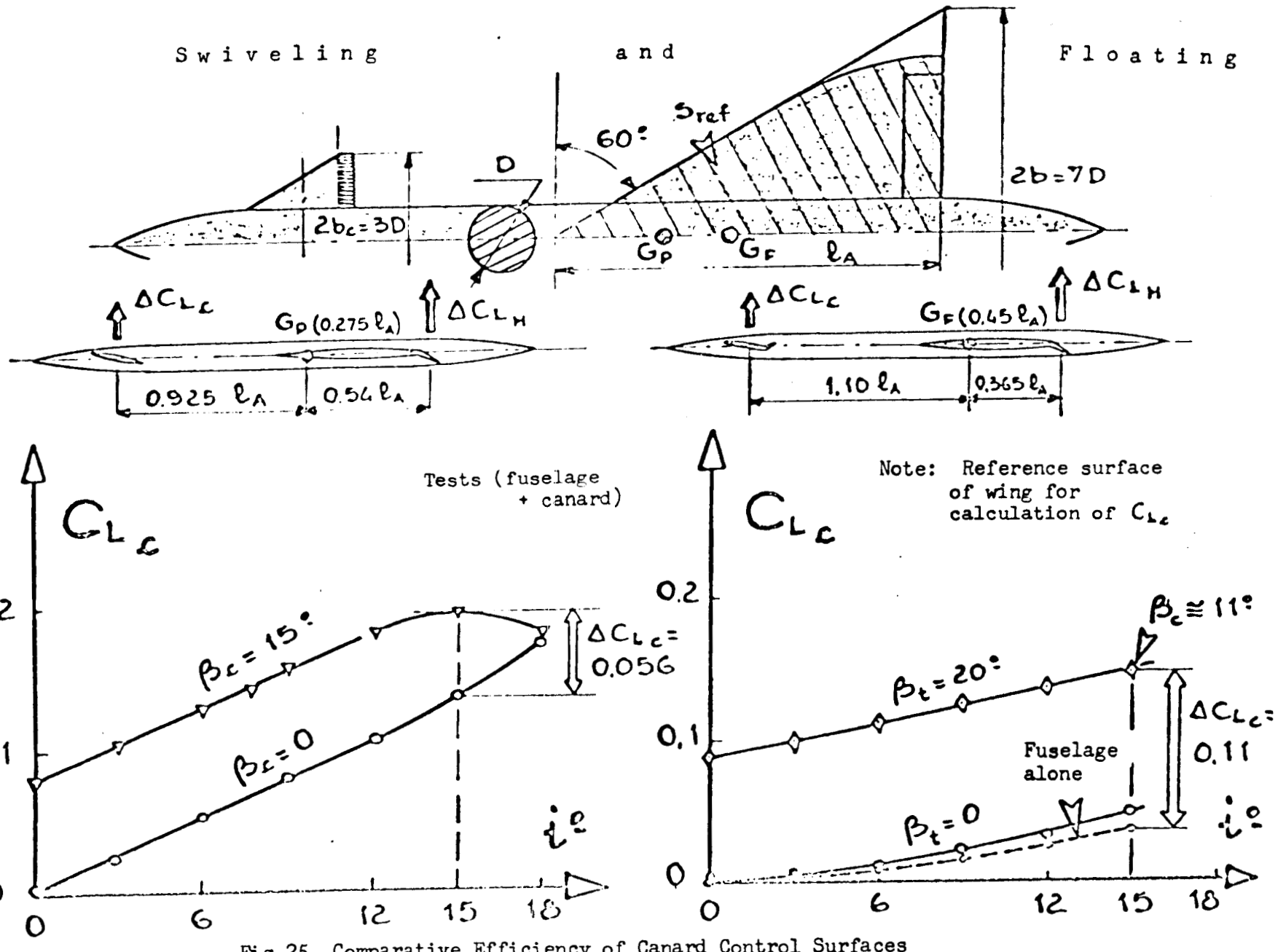

Fig.25 Comparative Efficiency of Canard Control Surfaces

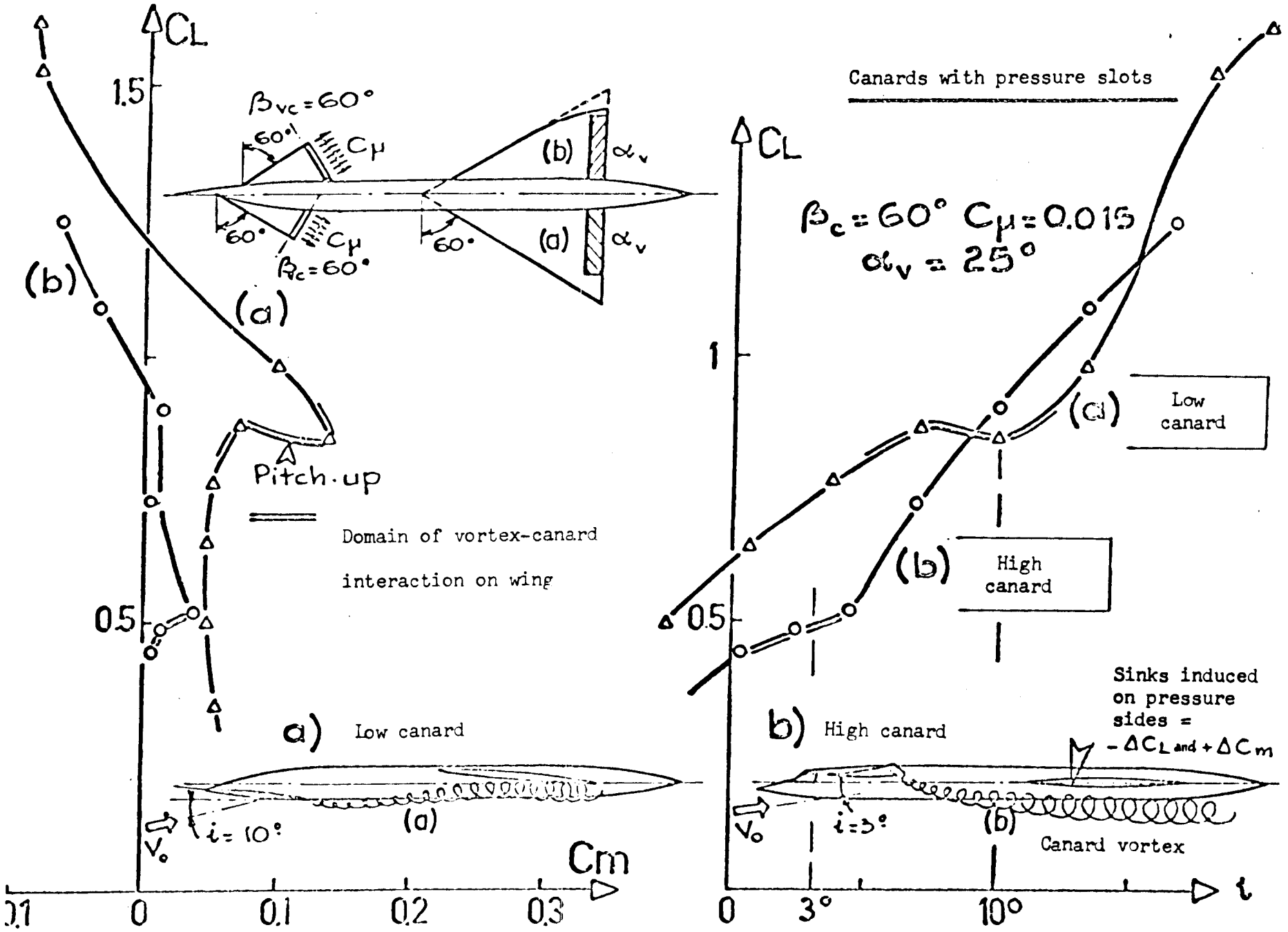

Fig.26 Longitudinal Perturbations with Canard Aircraft

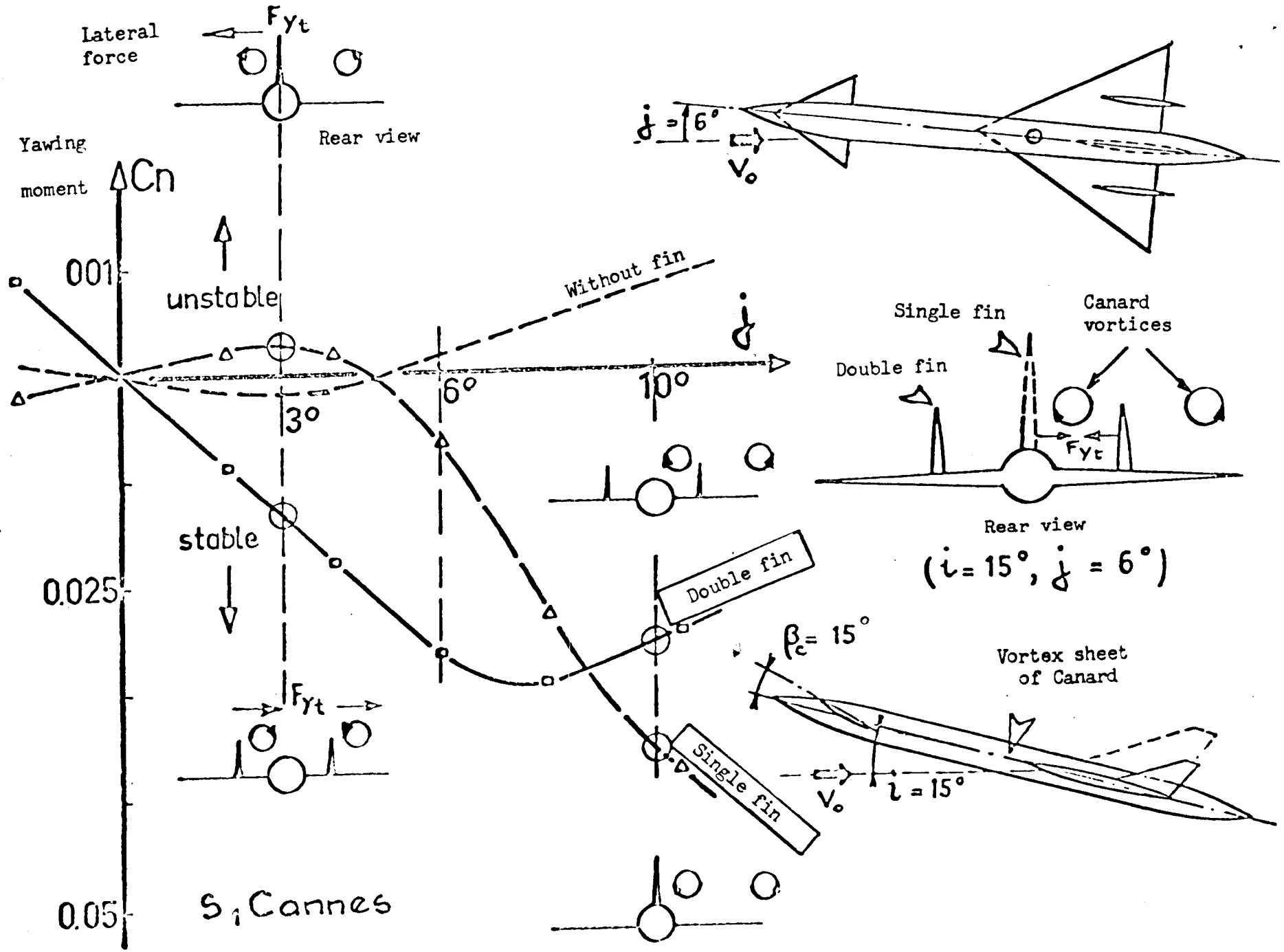

Fig.27 Transverse Perturbations with Canard Aircraft

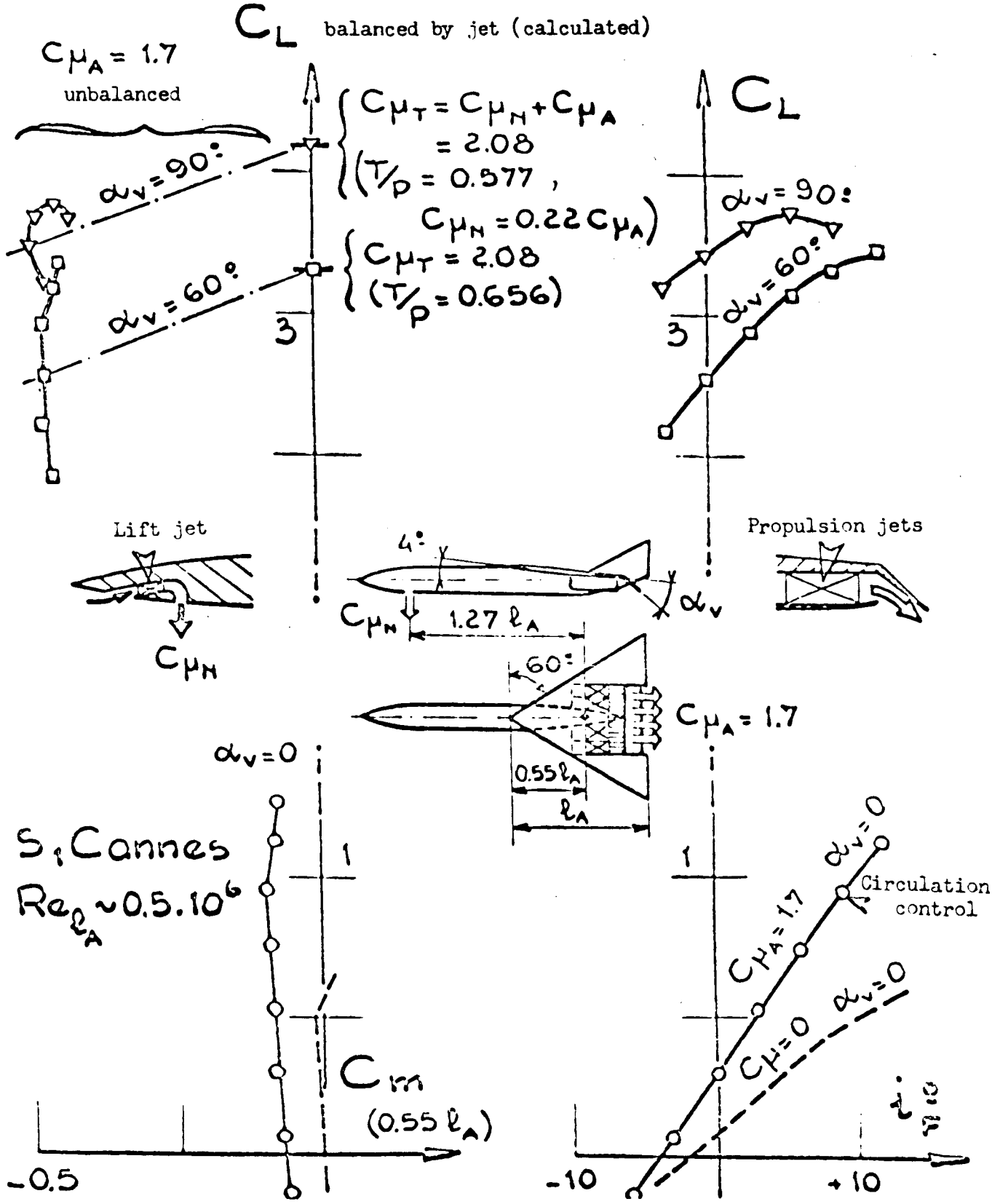

Fig.28 Longitudinal Balancing by Jet

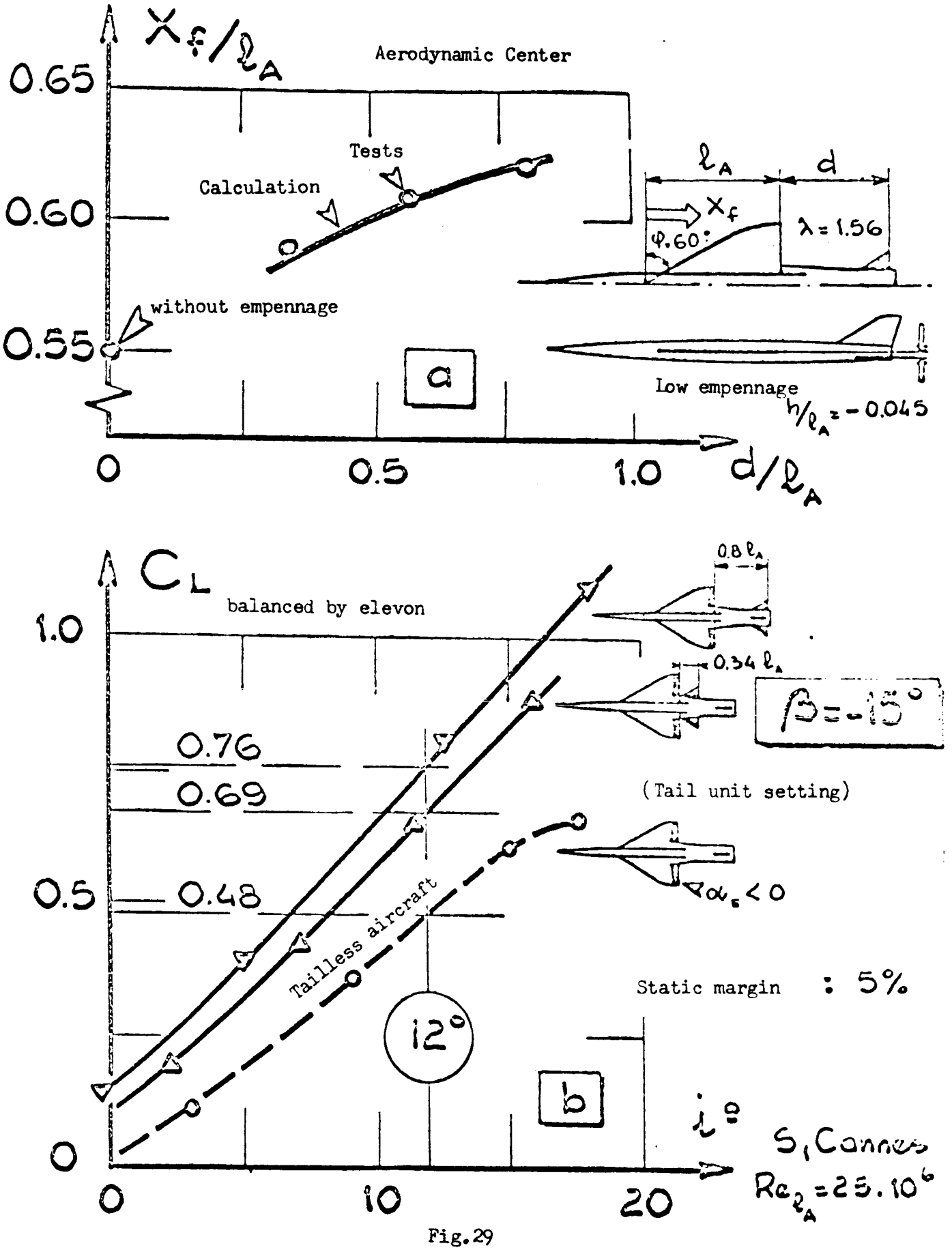
X_f/ℓ_A
Aerodynamic Center
0.65
0.60
0.55
Tests
Calculation
without empennage
ℓ_A
d
X_f
φ.60°
λ = 1.56
a
Low empennage
$h/\ell_A = -0.045$
0
0.5
1.0
d/ℓ_A
C_L
balanced by elevon
1.0
0.5
0
0.76
0.69
0.48
0.8 ℓ_A
0.34 ℓ_A
$\beta = -15°$
(Tail unit setting)
$\alpha_c < 0$
Tailless aircraft
12°
b
Static margin : 5%
i°
0
10
20
S, Cannes
$Re_{\ell_A} = 25.10^6$

Fig.29

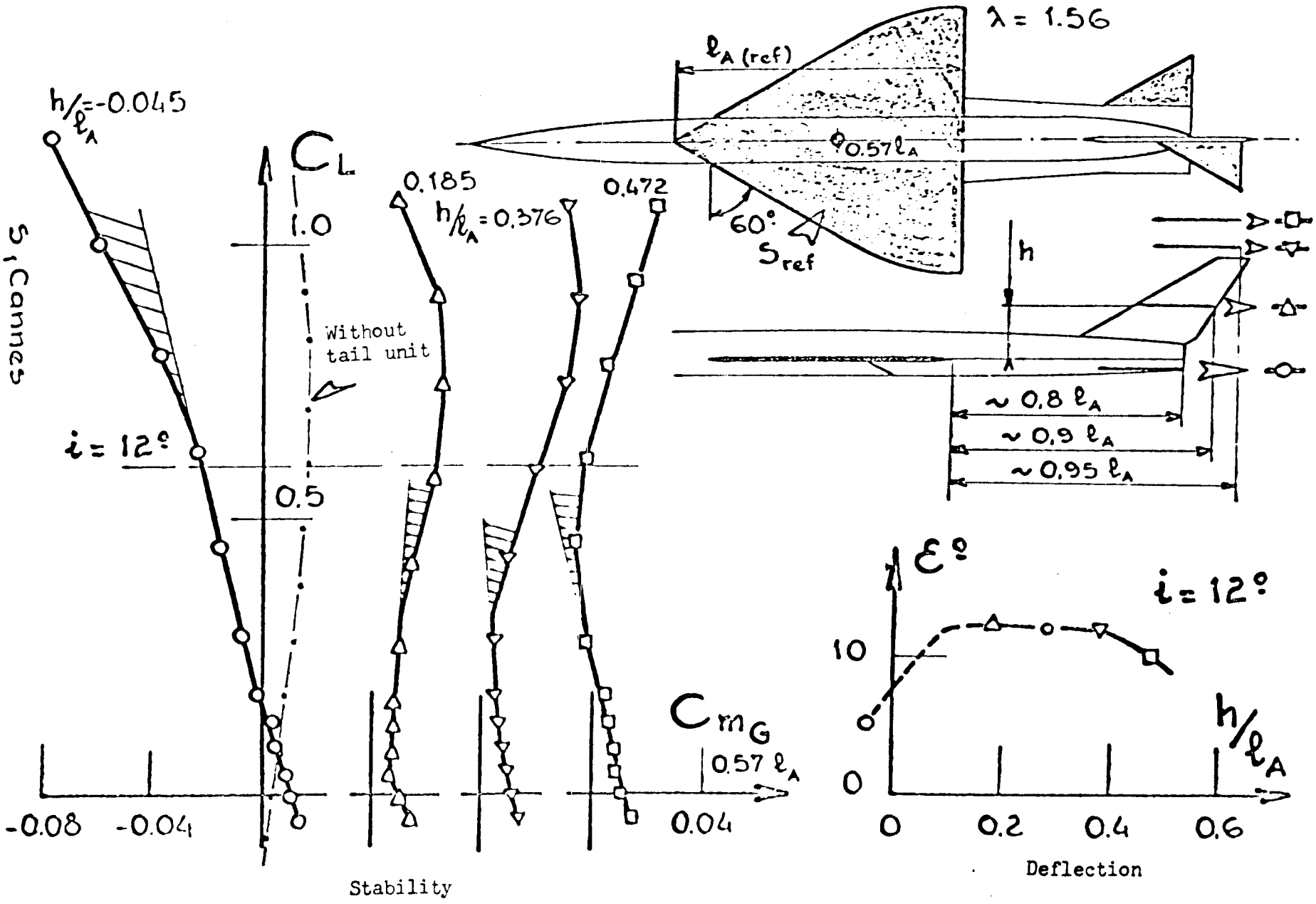
λ = 1.56
$\ell_{A\,(ref)}$
$\varphi_{0.57\ell_A}$
60°
S_{ref}
h
~ 0,8 ℓ_A
~ 0,9 ℓ_A
~ 0,95 ℓ_A
h/ℓ_A=-0.045
C_L
1.0
0.5
i = 12°
Without tail unit
0.185
h/ℓ_A=0.376
0.472
C_{mG}
0.57 ℓ_A
-0.08
-0.04
0.04
ε°
i = 12°
10
0
0
0.2
0.4
0.6
h/ℓ_A
Deflection
Stability
S.I.Cannes
63

Fig.30

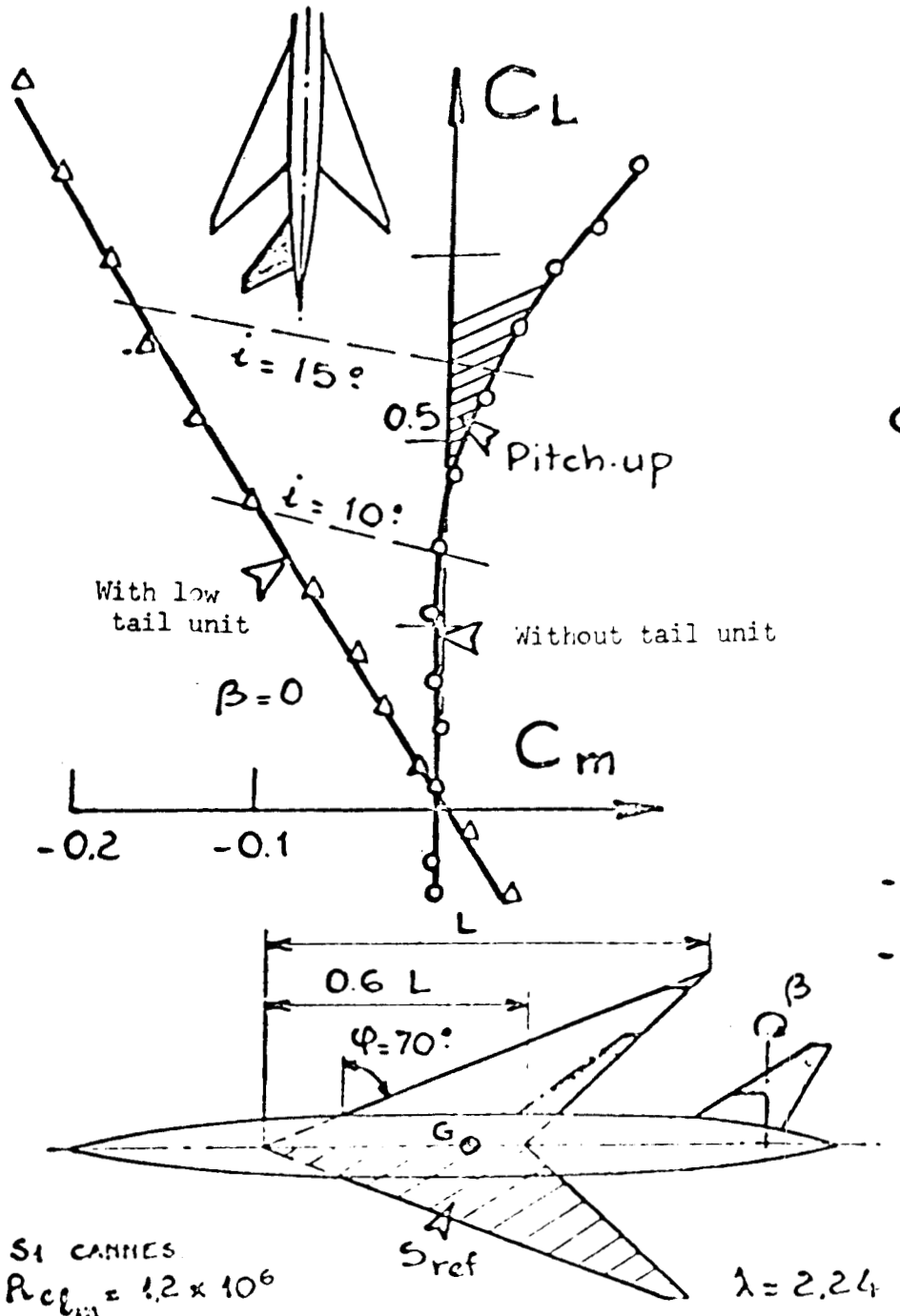
C_L
i = 15°
0.5
Pitch-up
i = 10°
With low tail unit
Without tail unit
β = 0
C_m
-0.2
-0.1
L
0.6 L
φ = 70°
β
G_0
S_{ref}
S1 CAMMES
$R_{e_{l_m}} = 1.2 \times 10^6$
λ = 2.24

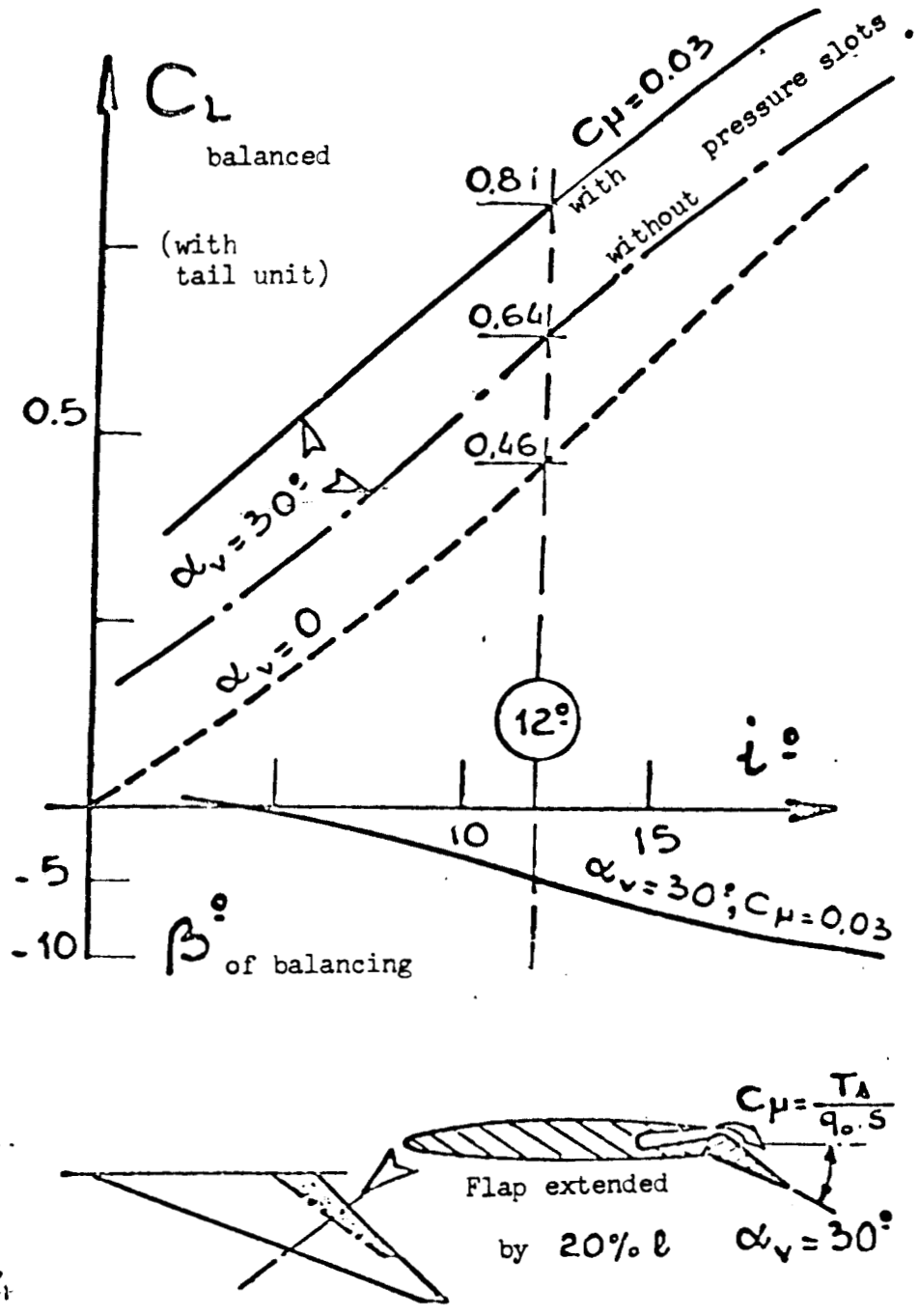
C_L
balanced
(with tail unit)
0.5
-5
-10
C_μ=0.03
0.8 i
with pressure slots
without
0.64
0.46
α_v=30°
α_v=0
12°
i°
10
15
α_v=30°; C_μ=0.03
β° of balancing
$C_\mu = \frac{T_A}{q_0 \cdot S}$
Flap extended by 20% l
α_v=30°

Fig.31

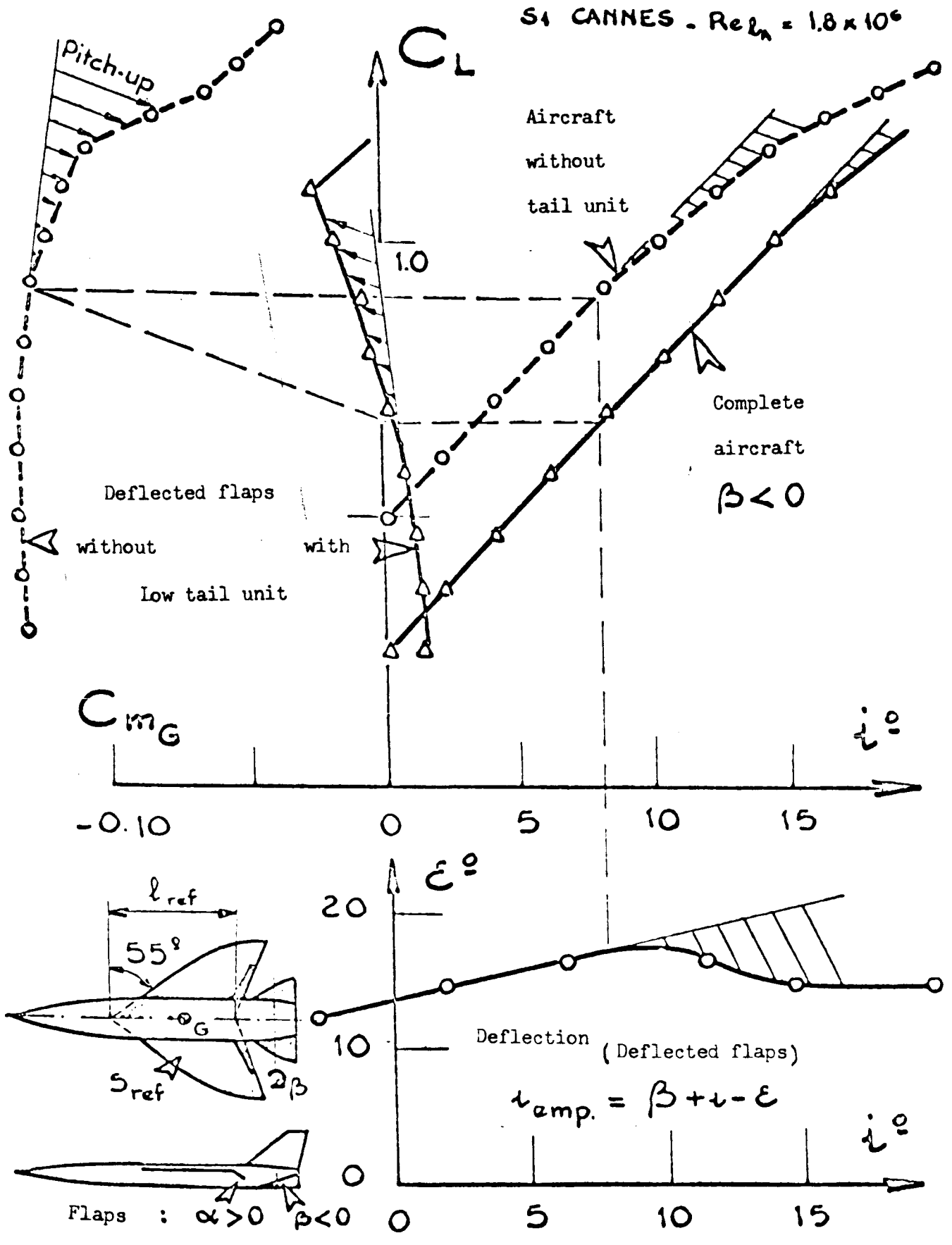
S1 CANNES - Re$_{l_m}$ = 1.8 x 10^6
Pitch-up
C_L
Aircraft
without
tail unit
1.0
Complete
aircraft
$\beta < 0$
Deflected flaps
without
with
Low tail unit
C_{m_G}
$i°$
-0.10
0
5
10
15
l_{ref}
55°
S_{ref}
2β
$\varepsilon°$
20
10
0
Deflection (Deflected flaps)
$i_{amp.} = \beta + i - \varepsilon$
Flaps : $\alpha > 0$ $\beta < 0$

Fig.32

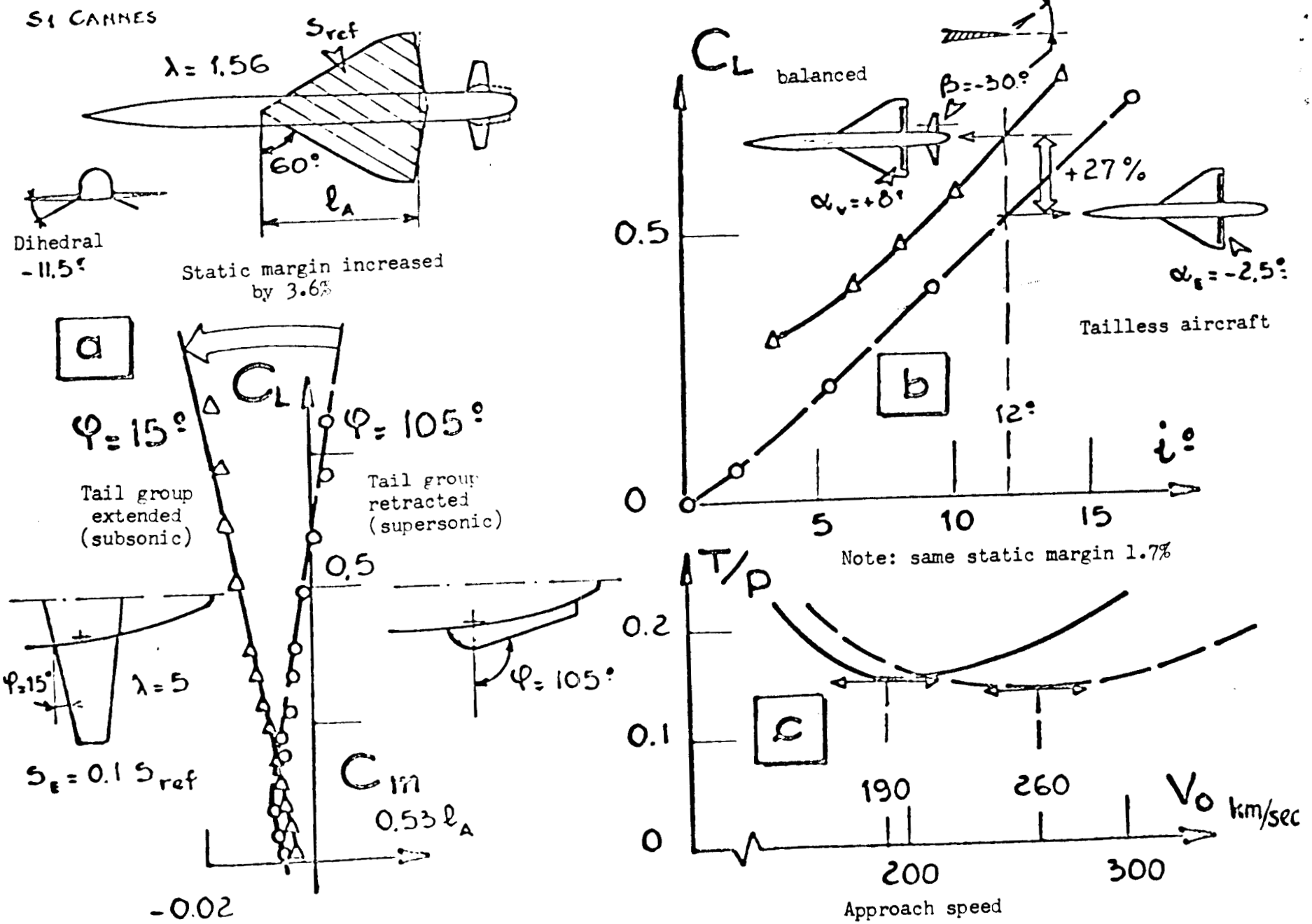
S1 CANNES
S_{ref}
$\lambda = 1.56$
60°
ℓ_A
Dihedral
-11.5°
Static margin increased
by 3.6%
a
C_L
$\varphi = 15°$
$\varphi = 105°$
Tail group
extended
(subsonic)
Tail group
retracted
(supersonic)
0.5
$\varphi = 15°$
$\lambda = 5$
$\varphi = 105°$
$S_E = 0.1\ S_{ref}$
C_{lm}
$0.53\ \ell_A$
-0.02
C_L
balanced
$\beta = -30°$
$\alpha_v = +8°$
+27%
$\alpha_E = -2.5°$
Tailless aircraft
b
0.5
0
12°
i°
5
10
15
Note: same static margin 1.7%
T/P
0.2
0.1
0
c
190
260
V_0 km/sec
200
300
Approach speed

Fig.33

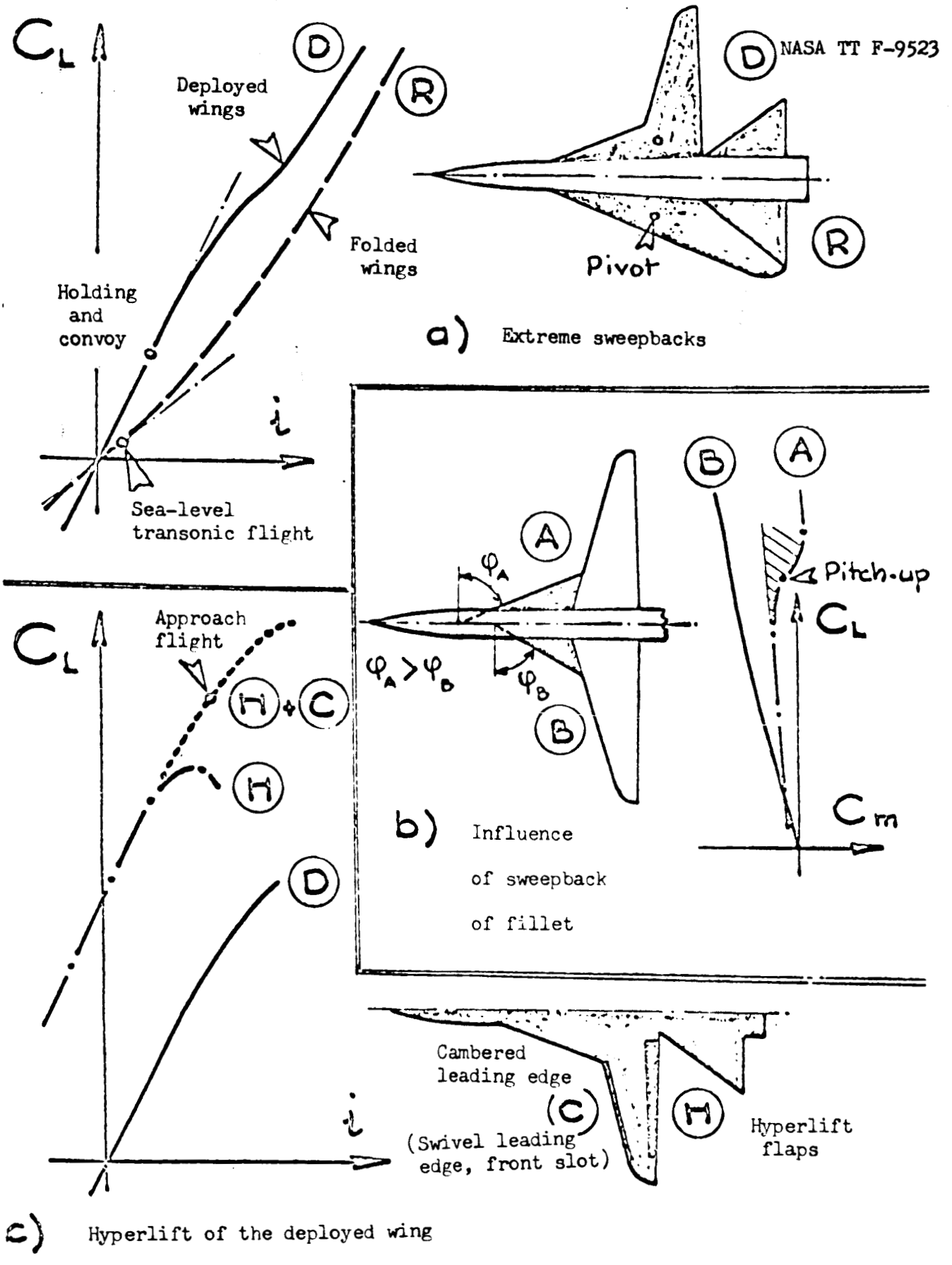

Fig.34 Principle of Variable-Sweep Aircraft